Article

Comparative Metabolic Study of *Tamarindus indica* L.'s Various Organs Based on GC/MS Analysis, *In Silico* and *In Vitro* Anti-Inflammatory and Wound Healing Activities

Shaza H. Aly [1] , Mahmoud A. El-Hassab [2] , Sameh S. Elhady [3,4] and Haidy A. Gad [5,6,*]

1   Department of Pharmacognosy, Faculty of Pharmacy, Badr University in Cairo, Cairo 11829, Egypt
2   Department of Medicinal Chemistry, Faculty of Pharmacy, King Salman International University (KSIU), South Sinai 46612, Egypt
3   Department of Natural Products, Faculty of Pharmacy, King Abdulaziz University, Jeddah 21589, Saudi Arabia
4   Center for Artificial Intelligence in Precision Medicines, King Abdulaziz University, Jeddah 21589, Saudi Arabia
5   Department of Pharmacognosy, Faculty of Pharmacy, Ain Shams University, Cairo 11566, Egypt
6   Department of Pharmacognosy, Faculty of Pharmacy, King Salman International University (KSIU), South Sinai 46612, Egypt
*   Correspondence: haidygad@pharma.asu.edu.eg

Abstract: The chemical composition of the *n*-hexane extract of *Tamarindus indica's* various organs—bark, leaves, seeds, and fruits (TIB, TIL, TIS, TIF)—was investigated using gas chromatography-mass spectrometry (GC/MS) analysis. A total of 113 metabolites were identified, accounting for 93.07, 83.17, 84.05, and 85.08 % of the total identified components in TIB, TIL, TIS, and TIF, respectively. Lupeol was the most predominant component in TIB and TIL, accounting for 23.61 and 22.78%, respectively. However, *n*-Docosanoic acid (10.49%) and methyl tricosanoate (7.09%) were present in a high percentage in TIS. However, α-terpinyl acetate (7.36%) and α-muurolene (7.52%) were the major components of TIF *n*-hexane extract. By applying a principal component analysis (PCA) and hierarchal cluster analysis (HCA) to GC/MS-based metabolites, a clear differentiation of *Tamarindus indica* organs was achieved. The anti-inflammatory activity was evaluated in vitro on lipopolysaccharide (LPS)-induced RAW 264.7 macrophages. In addition, the wound healing potential for the *n*-hexane extract of various plant organs was assessed using the in-vitro wound scratch assay using Human Skin Fibroblast cells. The tested extracts showed considerable anti-inflammatory and wound-healing activities. At a concentration of 10 µg/mL, TIL showed the highest nitric oxide (NO) inhibition by 53.97 ± 5.89%. Regarding the wound healing potential, after 24 h, TIB, TIL, TIS, and TIF *n*-hexane extracts at 10 g/mL reduced the wound width to 1.09 ± 0.04, 1.12 ± 0.18, 1.09 ± 0.28, and 1.41 ± 0.35 mm, respectively, as compared to the control cells (1.37 ± 0.15 mm). These findings showed that the *n*-hexane extract of *T. indica* enhanced wound healing by promoting fibroblast migration. Additionally, a docking study was conducted to assess the major identified phytoconstituents' affinity for binding to glycogen synthase kinase 3-β (GSK3-β), matrix metalloproteinases-8 (MMP-8), and nitric oxide synthase (iNOS). Lupeol showed the most favourable binding affinity to GSK3-β and iNOS, equal to -12.5 and -13.7 Kcal/mol, respectively, while methyl tricosanoate showed the highest binding affinity with MMP-8 equal to -13.1 Kcal/mol. Accordingly, the *n*-hexane extract of *T. indica's* various organs can be considered a good candidate for the management of wound healing and inflammatory conditions.

Keywords: *Tamarindus indica* L.; GC/MS; anti-inflammatory; wound healing; molecular docking; chemometric analysis; drug discovery; public health

1. Introduction

Tamarindus is a monospecific genus belonging to the Fabaceae family and usually has been identified under the name Tamarind [1]. *Tamarindus indica* Linn. is a tropical fruit tree that can be found growing wild in many tropical and subtropical areas [2]. Tamarind is a semi-deciduous tree, slow growing but long-lived, that can reach a height of up to 30 m. The leaves are alternate and paripinnate, and its fruit is a legume appearing as indehiscent pods with 1–10 seeds, which represent the main criteria of plants belonging to the Fabaceae family [3–6]. The fruit was especially well-known and commonly used by the ancient Egyptians and widely consumed and traded in Africa [3]. The fruit has usually been used in food dishes through different applications as a condiment and spice and could be eaten fresh or raw. Tamarind is sold as an entire pod, paste, or concentrate in speciality food stores all throughout the world [7,8]. Its fruit has been reported in the literature for its pharmacological antioxidant, anti-inflammatory, antidiabetic, anti-Alzheimer, and antihyperlipidemic properties [9–11]. Tamarind has been commonly used in folk medicine for the treatment of diarrhoea and dysentery, helminth infections, fever, and abdominal pain. It is also used as an anti-malarial and laxative and has a role in wound healing [3]. Traditional Indian and African medicine has made substantial use of different tamarind products, including its leaves, fruit, and seeds [12]. Across many areas of central West Africa, tamarind leaves and bark are used traditionally to alleviate wounds [3,13]. Leaves of Tamarind have nutritional value due to their richness in vitamins and minerals [12]. Its leaves have exhibited potential antioxidant, antibacterial and antifungal, anti-inflammatory, and analgesic activities [14–17]. Additionally, the leaves of Tamarind have an anti-inflammatory role in Indian folk medicine [18].

Regarding the bark, it is effective as an astringent and tonic agent in lotions or poultices to relieve sores, ulcers, boils, and rashes, owing to its richness with tannins [12]. In addition, the bark showed in vivo antihyperglycemic, anti-inflammatory, and analgesic activities [17,19]. Moreover, leaves and bark have been reported for their anthelmintic activity [20].

Wound healing is a normal complex repair process that requires synchronisation between various biological and immunological systems, including many phases of inflammation, proliferation, and contraction of the wound, with the formation of granulation tissues and remodelling [21–23]. Plants and plant products, such as *Aloe vera*, *Sophora flavescens*, *Punica granatum* L., *Mimosa pudica* L., and *Hibiscus rosa sinensis* L., have been used in traditional medicine to cure and prevent diseases, especially wounds [24–26].

Recently, there has been a great demand for the development of natural products to cure different conditions owing to their safety, availability, versatile biological activities, and unique secondary metabolites [27–31]. Consequently, the exploration of medicinal plants as new candidates for wound healing would be valuable and beneficial, especially medicinal plants that are characterised by biocompatibility, wound healing, and anti-inflammatory properties [22,23,32,33]. Many reports have revealed that using *n*-hexane as an extracting solvent targets non-polar compounds [21,34,35], and many studies have proven the role of *n*-hexane extract from various plants in anti-inflammatory and wound healing conditions [36–39].

Thus, the purpose of this present study was to compare and determine the chemical composition of the *n*-hexane extract of *T. indica* L.'s various organs using GC/MS analysis. Further, the principal component analysis (PCA) and hierarchical cluster analysis (HCA) were applied to discriminate among various plant organs based on their chemical profiles, which could be used as a tool for the detection of similarities and differences among the four organs. Furthermore, the *n*-hexane extract obtained from *T. indica* L.'s various organs were investigated for their anti-inflammatory and wound healing properties for the first time along with a molecular docking study to correlate the chemical composition with the mentioned biological activity. To the best of our knowledge, this is the first study on the wound-healing properties for the various organs of *T. indica* L. *n*-hexane extract.

2. Results and Discussion

2.1. GC/MS Analysis of the N-Hexane Extract of Tamarindus indica L. Various Organs

The chemical composition of the *n*-hexane extract of *T. indica*, bark, leaves, seeds, and fruit (TIB, TIL, TIS, and TIL) were investigated using GC/MS analyses (Table 1). The yields of extraction of TIB, TIL, TIS, and TIL using *n*-hexane were 4.20, 6.10, 2.07, and 3.12% *w/w*, respectively. The samples encompassed 113 constituents that accounted for 93.07, 83.17, 84.05, and 85.08 % of the total identified components in bark, leaves, seeds, and fruits of *T. indica*, respectively. The major constituents identified in the *n*-hexane extract of TIB were lupeol (23.61%), lupeol acetate (23.02%), lupenone (9.36%), *n*-tetratriacontane (8.16%), 24-methylenecycloartanol (5.87%), 1-heptatriacontanol (4.25%), and *γ*-sitosterol (4.17%). Regarding the *n*-hexane extract of TIL, lupeol (22.78%), lupenone (13.08%), *γ*-sitosterol (8.83%), (17*E*)-Cholesta-17,24-diene-3,6-diol (8.23%), *n*-nonacosane (4.13%), Betulinaldehyde (3.70%), and *β*-Amyrone (2.05%) were characterised as the chief metabolites. In this case, lupenone and lupeol were present in higher percentages as compared to other organs. Moreover, *n*-Docosanoic acid (10.49%), methyl tricosanoate (7.09%), tetracosanal (5.42%), 2-methylhexacosane (4.31%), 11-methylpentacosane (4.22%), and heneicosyl acetate (2.94%) displayed the highest percentages in the *n*-hexane extract of TIS. Additionally, among the major constituents, especially in TIS, are *n*-octacosane (4.63%), *n*-heptacosane (4.17%), *cis*-13,16-docosadienoic acid (3.70%), *n*-hexacosane (2.47%), *n*- pentacosane (2.46%), and methyl tetracosanoate (2.17%). Furthermore, the *n*-hexane extract of TIF showed a predominantly high percentage of *α*-terpinyl acetate (7.36%), *α*-muurolene (7.52%), 2-methyl hexadecane (5.70%), methyl pentadecanoate (4.53%), *α*-eicosene (3.44%), and linolenic acid (3.26%) in addition to chief constituents *n*-heptacosane (6.67%), *n*-nonacosane (5.42%), squalene (4.17%), *cis*-13,16-docosadienoic acid (3.76%), lupeol (3.76%), *n*-tetratriacontane (3.38%), and hentriacontane (3.32%). It was notable that *γ*-sitosterol is the chief component in the four organs ranging from (3.79%) in TIS to (11.28%) in TIF. It was notable that squalene, n-nonacosane, n-hentriacontane, 5*α*-stigmast-22-en-3*β*-ol, and *γ*-sitosterol were detected in the four organs. The major compounds present in the four various organs of *T. indica* are represented in (Figure 1).

Table 1. Chemical profile of *n*-hexane extract from various organs of *T. indica*: TIB (bark), TIL (leaves), TIS (seeds), and TIF (fruits) using GC/MS analysis.

No.	R_t (min)	Compound Name	$RI_{Exp.}$ [a]	RI_{Lit} [b]	Molecular Formula	Peak Area (%)			
						TIB	TIL	TIS	TIF
1	6.94	*α*-pinene	930	930	$C_{10}H_{16}$	-	-	-	0.38
2	8.16	*α*-Sabinene	971	971	$C_{10}H_{16}$	-	-	-	0.57
3	9.90	D-Limonene	1028	1028	$C_{10}H_{16}$	-	-	-	1.35
4	9.97	1,8-Cineole	1030	1030	$C_{10}H_{18}O$	-	-	-	0.61
5	13.93	Isoborneol	1156	1156	$C_{10}H_{18}O$	-	-	-	0.87
6	19.00	*α*-Terpinyl acetate	1328	1327	$C_{12}H_{20}O_2$	0.03	-	-	7.36
7	23.59	*α*-Muurolene	1494	1494	$C_{15}H_{24}$	0.04	-	-	7.52
8	27.69	2-Methylhexadecane	1668	1666	$C_{17}H_{36}$	0.03	-	-	5.70
9	31.07	Hexadecanal; Palmitaldehyde	1810	1811	$C_{16}H_{32}O$	-	-	-	0.36
10	31.25	Methyl pentadecanoate	1819	1820	$C_{16}H_{32}O_2$	-	-	-	4.53
11	31.52	Neophytadiene	1833	1837	$C_{20}H_{38}$	-	0.2	-	-
12	31.67	Hexahydrofarnesyl acetone	1841	1842	$C_{18}H_{36}O$	-	0.09	-	-
13	32.43	Heptadecan-2-one	1880	1892	$C_{17}H_{34}O$	0.03	0.07	-	-
14	33.37	Methyl palmitate	1928	1928	$C_{17}H_{34}O_2$	0.11	-	-	-
15	34.42	*α*-Eicosene	1980	1986	$C_{20}H_{40}$	-	-	-	3.44
16	35.62	Octadecanal	2040	2034	$C_{18}H_{36}O$	-	-	0.58	-
17	36.73	n-Heneicosane	2098	2100	$C_{21}H_{44}$	0.05	-	-	-
18	36.85	Methyl linolenate	2104	2108	$C_{19}H_{32}O_2$	0.07	-	-	-
19	37.06	Phytol	2116	2116	$C_{20}H_{40}O$	-	1.97	-	-
20	37.32	Linolenic acid	2130	2134	$C_{18}H_{30}O_2$	-	-	1.23	3.26
21	37.88	Ethyl linolate	2160	2164	$C_{20}H_{36}O_2$	0.08	-	-	-
22	38.48	Stearic acid=n-Octadecanoic acid	2192	2180	$C_{18}H_{36}O_2$	-	-	0.64	-
23	38.59	n-Docosane	2198	2200	$C_{22}H_{46}$	0.07	-	0.82	-
24	38.89	Phytol acetate	2215	2218	$C_{22}H_{42}O_2$	-	-	0.67	-
25	39.17	Methyl nonadecanoate	2231	2230	$C_{20}H_{40}O_2$	-	-	0.59	-
26	40.12	Heneicosan-3-one	2285	2283	$C_{21}H_{42}O$	-	-	0.54	-
27	40.20	1-Eicosanol	2289	2292	$C_{20}H_{42}O$	0.09	-	-	-
28	40.36	n- Tricosane	2298	2300	$C_{23}H_{48}$	0.17	0.04	-	-
29	40.65	Methyl cis-11-eicosenoate	2315	2302	$C_{21}H_{40}O_2$	-	-	1.83	-

Table 1. *Cont.*

No.	R_t (min)	Compound Name	$RI_{Exp.}$ [a]	RI_{Lit} [b]	Molecular Formula	Peak Area (%)			
						TIB	TIL	TIS	TIF
30	41.15	Methyl eicosanoate	2344	2339	$C_{21}H_{42}O_2$	-	-	0.77	-
31	41.41	4,8,12,16-Tetramethylheptadecan-4-olide	2360	2364	$C_{21}H_{40}O_2$	-	0.07	0.40	-
32	41.57	n-Eicosanoic acid	2369	2380	$C_{20}H_{40}O_2$	-	-	1.01	-
33	42.07	2,2′-Methylene-bis-(6-tert butyl-4-methylphenol)	2398	2398	$C_{23}H_{32}O_2$	0.10	0.06	-	-
34	42.24	n-Tetracosane	2409	2400	$C_{24}H_{50}$	-	-	0.53	-
35	42.48	Docosanal	2424	2426	$C_{22}H_{44}O$	-	-	0.64	1.48
36	42.61	Methyl heneicosanoate	2431	2430	$C_{22}H_{44}O_2$	0.07	-	-	-
37	42.85	1-Docosanol	2446	2456	$C_{22}H_{46}O$	-	-	0.54	-
38	43.1	2-Methyltetracosane	2461	2465	$C_{25}H_{52}$	-	-	1.28	-
39	43.48	1-Pentatricosene	2484	2485	$C_{35}H_{70}$	-	-	1.77	-
40	43.62	Cyclogallipharaol	2493	2499	$C_{21}H_{36}O$	0.35	-	0.81	0.72
41	43.70	n- Pentacosane	2498	2500	$C_{25}H_{52}$	0.24	0.23	2.46	-
42	43.87	Heneicosyl acetate	2509	2509	$C_{23}H_{46}O_2$	-	-	2.94	-
43	43.96	Palmitic acid β-monoglyceride	2514	2519	$C_{19}H_{38}O_4$	0.07	-	-	-
44	44.230	Methyl docosanoate	2531	2531	$C_{23}H_{46}O_2$	0.08	-	-	-
45	44.305	11-Methylpentacosane	2536	2529	$C_{26}H_{54}$	-	-	4.22	-
46	44.675	cis-13,16-Docasadienoic acid	2560	2566	$C_{22}H_{40}O_2$	-	-	3.70	3.76
47	44.84	n-Docosanoic acid	2570	2569	$C_{22}H_{44}O_2$	-	-	10.49	-
48	45.18	Ethyl docosanoate	2592	2593	$C_{24}H_{48}O_2$			1.44	
49	45.275	n-Hexacosane	2598	2600	$C_{26}H_{54}$	0.11	0.20	2.47	-
50	45.43	Methyl tricosanoate	2608	2615	$C_{24}H_{48}O_2$	-	-	7.09	-
51	45.62	Erucylamide	2621	2625	$C_{22}H_{43}NO$	-	-	1.32	-
52	45.83	Tetracosanal	2635	2632	$C_{24}H_{48}O$	-	-	5.42	-
53	46.19	2-Methylhexacosane	2658	2662	$C_{27}H_{56}$	-	-	4.31	-
54	46.793	1-Heptacosene	2698	2694	$C_{27}H_{54}$	0.58	-	-	-
55	46.805	n-Heptacosane	2699	2700	$C_{27}H_{56}$	-	1.37	4.17	6.67
56	47.310	Methyl tetracosanoate	2733	2731	$C_{25}H_{50}O_2$	0.14	-	2.17	-
57	47.77	2-Methylheptacosane	2765	2761	$C_{28}H_{58}$	-	-	0.59	-
58	48.02	16-Acetoxycarterochaetol	2782	2787	$C_{22}H_{36}O_3$	-	-	0.26	-
59	48.260	n-Octacosane	2798	2800	$C_{28}H_{58}$	0.09	0.44	4.63	-
60	48.800	Squalene	2836	2835	$C_{30}H_{50}$	0.24	1.29	1.82	4.17
61	48.865	n-Hexacosanal	2841	2833	$C_{26}H_{52}O$	0.04	0.09	-	-
62	48.94	n-Hexacosanol	2846	2848	$C_{26}H_{54}O$	-	-	0.25	-
63	49.26	2-Methyloctacosane	2869	2860	$C_{29}H_{60}$	-	-	1.32	-
64	49.44	1-Nonacosene	2882	2884	$C_{29}H_{58}$	-	-	0.67	-
65	49.730	n-Nonacosane	2902	2900	$C_{29}H_{60}$	1.26	4.13	1.69	5.42
66	50.175	15-Methylnonacosane	2935	2931	$C_{30}H_{62}$	0.03	-	-	-
67	50.285	Methyl hexacosanoate	2943	2940	$C_{27}H_{54}O_2$	-	0.17	-	-
68	50.515	2-Methylnonacosane	2960	2960	$C_{30}H_{62}$	0.04	-	-	-
69	51.040	n-Triacontane	2998	3000	$C_{30}H_{62}$	0.04	0.37	-	-
70	51.130	Benzyl icosanoate	3005	3003	$C_{27}H_{46}O_2$	0.02	-	-	-
71	51.210	1-Heptacosanol	3011	3016	$C_{27}H_{56}O$	-	0.06	-	-
72	51.655	n-Octacosanal	3045	3039	$C_{28}H_{56}O$	-	0.29	-	0.44
73	51.850	2-Methyltriacontane	3059	3060	$C_{31}H_{64}$	-	0.09	-	-
74	52.370	n-Hentriacontane	3099	3100	$C_{31}H_{64}$	0.08	1.73	0.61	3.32
75	52.475	Octacosanol	3107	3110	$C_{28}H_{58}O$	1.02	-	-	1.89
76	52.72	13-Methylhentriacontane	3126	3130	$C_{32}H_{66}$	-	0.15	0.85	-
77	52.835	Campesterol	3134	3131	$C_{28}H_{48}O$	-	0.05	-	-
78	53.015	Cholest-3,5-diene	3148	-	$C_{27}H_{44}$	0.07	0.09	-	-
79	53.085	α-Tocopherol	3154	3149	$C_{29}H_{50}O_2$	0.03	1.01	-	-
80	53.155	Ergosta-5,8,22-trien-3-ol, (3β,22E)-	3159	3158	$C_{28}H_{44}O$	-	0.40	-	-
81	53.340	Stigmasterol	3173	3170	$C_{29}H_{48}O$	0.11	0.25	-	-
82	53.475	β-Sitosterol	3183	3197	$C_{29}H_{50}O$	-	0.10	-	-
83	53.710	n-Dotriacontane	3201	3200	$C_{32}H_{66}$	0.26	0.23	-	-
84	53.925	Cholest-5-ene, 3β-methoxy	3216	3216	$C_{28}H_{48}O$	-	0.08	-	-
85	54.375	Triacontanal	3248	3251	$C_{30}H_{60}O$	-	0.47	-	0.69
86	54.575	5α-Stigmast-22-en-3β-ol	3261	3253	$C_{29}H_{50}O$	1.09	0.84	0.72	1.39
87	55.070	Chondrillasterol	3296	3295	$C_{29}H_{48}O$	1.42	0.07	-	-
88	55.130	n-Tritriacontane	3300	3300	$C_{33}H_{68}$	-	0.41	-	-
89	55.230	Lanosterol	3306	3302	$C_{30}H_{50}O$	0.25	0.13	-	-
90	55.310	1-Triacontanol	3311	3306	$C_{33}H_{68}O$	0.38	-	-	-
91	55.440	5α-Stigmastan-3β-ol	3320	3325	$C_{29}H_{52}O$	0.04	0.14	-	-
92	55.655	β-Amyrin	3332	3337	$C_{30}H_{50}O$	0.11	-	-	-
93	56.015	γ-Sitosterol	3353	3351	$C_{29}H_{50}O$	4.17	8.83	3.79	11.28
94	56.200	2-Methyldotriacontane	3364	3259	$C_{33}H_{68}$	-	0.52	-	0.76
95	56.335	β-Amyrone	3372	3327	$C_{30}H_{50}O$	1.78	2.05	-	-
96	56.445	α-Amyrin	3379	3376	$C_{30}H_{50}O$	-	0.33	-	-
97	56.740	n-Tetratriacontane	3397	3403	$C_{34}H_{70}$	8.16	1.21	-	3.38
98	57.020	β-Amyrin acetate	3446	3437	$C_{32}H_{52}O_2$	-	0.08	-	-
99	57.195	Lupenone	3488	3384	$C_{30}H_{48}O$	9.36	13.08	-	-
100	57.550	Lupeol acetate	3518	3525	$C_{32}H_{52}O_2$	23.02	1.68	-	-
101	57.68	Lupeol	3527	3500	$C_{30}H_{50}O$	23.61	22.78	-	3.76
102	58.015	(17E)-Cholesta-17,24-diene-3,6-diol	3550	-	$C_{27}H_{44}O_2$	0.29	8.23	-	-
103	58.170	Hexadecanoic acid, 3,7,11,15-tetramethyl-2-hexadecenyl ester	3561	3567	$C_{36}H_{70}O_2$	0.04	-	-	-
104	58.295	24-Methylenecycloartan-3-one	3570	-	$C_{31}H_{50}O$	0.45	-	-	-

Table 1. *Cont.*

No.	R_t (min)	Compound Name	RI_Exp.[a]	RI_Lit [b]	Molecular Formula	Peak Area (%)			
						TIB	TIL	TIS	TIF
105	58.605	24-Methylenecycloartanol	3591	-	$C_{31}H_{52}O$	5.87	0.18	-	-
106	58.890	3β-Hydroxystigmast-5-en-7-one	3611	3609	$C_{29}H_{48}O_2$	-	1.03	-	-
107	59.095	Betulinaldehyde	3625	3628	$C_{30}H_{48}O_2$	-	3.70	-	-
108	59.440	Germanicol	3649	-	$C_{30}H_{50}O$	-	0.80	-	-
109	61.000	Betulin	3757	3760	$C_{30}H_{50}O_2$	1.78	-	-	-
110	62.04	Ursane-3,12-diol	3829	-	$C_{30}H_{52}O_2$	-	0.59	-	-
111	62.11	1-Heptatriacontanol	3834	-	$C_{37}H_{76}O$	4.25	-	-	-
112	62.39	Stigmastane-3,6-dione	3853	3601	$C_{29}H_{48}O_2$	1.16	-	-	-
113	62.79	9,19-Cyclolanost-23-ene-3,25-diol, (3β,23E)-	3881	-	$C_{32}H_{52}O_3$	-	0.70	-	-
		Monoterpene Hydrocarbon				-	-	-	2.30
		Oxygenated Monoterpene				0.03	-	-	8.84
		Sesquiterpene Hydrocarbon				0.04	-	-	7.52
		Oxygenated Sesquiterpene				-	0.09	-	-
		Diterpenoids				-	2.24	1.33	-
		Triterpenoids				61.06	47.41	1.82	7.93
		Steroids				13.47	11.86	4.51	12.67
		Fatty acids and fatty acids derivatives				0.97	8.40	35.22	11.55
		Straight-chain Hydrocarbons and derivatives				12.77	12.1	40.36	33.55
		Others				4.73	1.07	0.81	0.72
		Total identified compounds %				93.07	83.17	84.05	85.08

Compounds listed in order of their elution in RTX-5 GC column. Identification was based on comparison of the compound mass spectral data (MS) and retention indices (RI) with those of NIST Mass Spectral Library (2011), Wiley Registry of Mass Spectral Data 8th edition and literature. [a] Retention index calculated experimentally in RTX-5 column relative to n-alkane series (C8–C28). [b] Published retention indices.
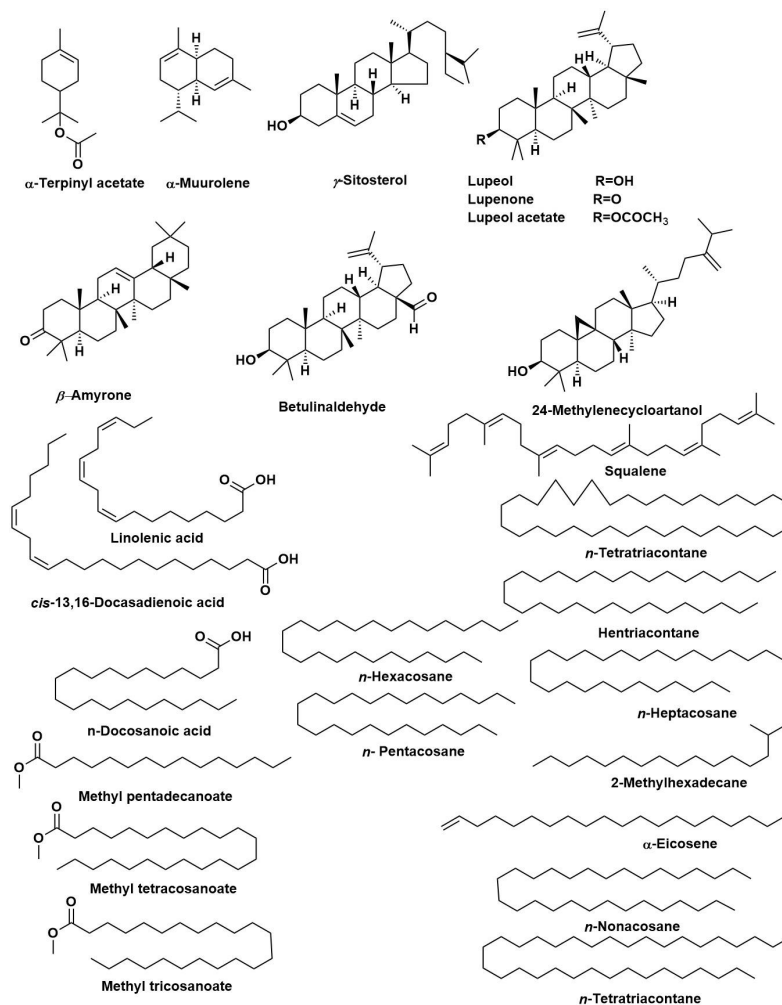
Figure 1. The major compounds identified in bark, leaves, seeds, and fruits of *Tamarindus indica*.

Triterpenoids and steroids are the predominant classes in the *T. indica* bark *n*-hexane extract, accounting for 61.06 % and 13.47%, respectively. Additionally, the *n*-hexane extract of *T. indica* leaves showed a high percentage of triterpenoids and steroids, representing 47.41% and 11.86% of the identified compounds, respectively, along with fatty acids and their derivatives accounting for 8.40 %. On the other hand, the most predominant classes of metabolites in the *n*-hexane extract of *T. indica* seeds were fatty acids and their derivatives and the straight-chain hydrocarbons, accounting for 35.22% and 40.36%, respectively. Meanwhile, the straight-chain hydrocarbons were the dominant class in the *n*-hexane extract of *T. indica* fruits, representing 33.55% of the total identified compounds, followed by steroids and fatty acids and their derivatives, accounting for 12.67% and 11.55%, respectively. The illustration of the metabolite distribution in the various organs of *T. indica* is represented in (Figure 2).
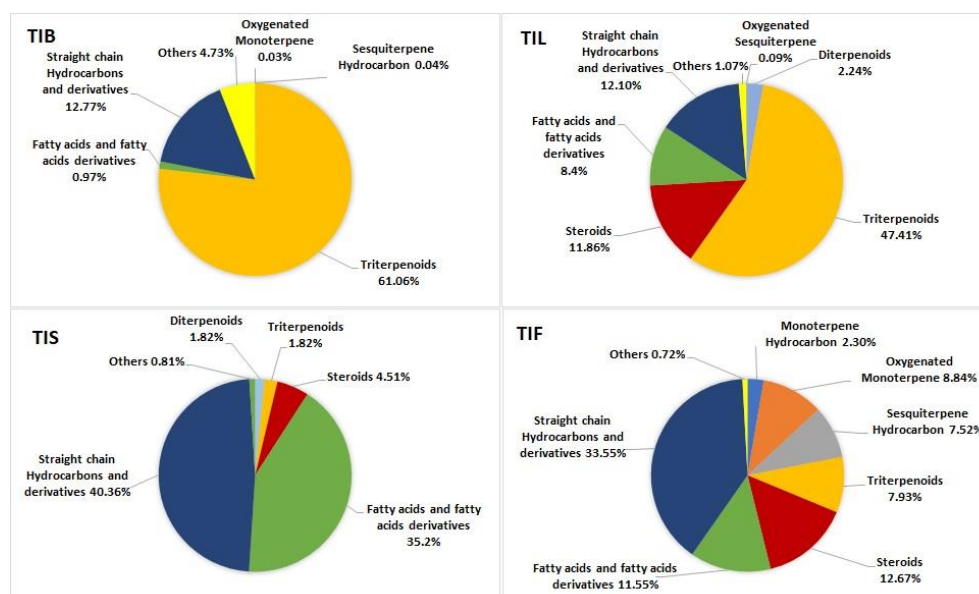
Figure 2. Pie charts demonstrate distribution of metabolite classes in percentages within various organs: TIB (bark), TIL (leaves), TIS (seeds), and TIF (fruits) of *Tamarindus indica*.

The fatty acids previously identified in the seeds of Tamarind from Sudan by Ibrahim et al. [40] were characterised as palmitic acid, oleic acid, and eicosanoic acid in addition to the identification of *β*-amyrin, *β*-sitosterol, and campesterol. *Cis*-vaccenic acid, 2-methyltetracosane, *β*-sitosterol, 9,12-octadecadienoic acid (*Z, Z*)-, and n-hexadecanoic acid were reported as the major metabolites identified in the oil of *T. indica* seeds collected from Nigeria. Another study by Carasek and Pawliszyn [41] reported that the volatile compounds in the tamarind fruit collected from Brazil included phenylacetaldehyde and furfural. Aldehyde and ester compounds were mostly identified by using Solid-Phase Microextraction (SPME) Fibres. It is important to note that the plant extract components can be influenced by variables including geographic, climatic, seasonal, and experimental settings. However, the aim of our study was to explore the difference in discriminating among the various organs of *T. indica*, not to study the effects of the above-mentioned variables from Gad et al. [42].

2.2. Chemometric Analysis Based on GC/MS Analysis

GC/MS-based metabolites showed both qualitative and quantitative variation among different *Tamarindus indica* organs. Consequently, chemometric analysis, representing both principal component analysis (PCA) and hierarchal cluster analysis (HCA), was applied to the relative peak areas of all the identified compounds of different *T. indica* organs to explore the similarities and differences among them. The PCA score plot and loading plot are shown in Figure 3a,b. In the PCA score plot, the percentage of the first two principal

components explained 83% of the variance in the data, where PC1 accounted for 63%, while PC2 explained only 20% of the data discrepancies. From the score plot, various *T. indica* organs were divided into four main groups, and each part was scattered in a separate quadrant. TIL and TIB were positioned on the positive side of PC1, whereas, TIF and TIS were located on the negative side of PC1. An in-depth inspection of the loading plot (Figure 3b) revealed that lupeol acetate was the major discriminating marker for TIB. Although lupeol was the major identified component in both TIB and TIL, it was ©dentified as the main segregating marker for TIL in addition to lupenone.

Figure 3. Principal component analysis score plot (**a**), loading plot (**b**), HCA dendrogram (**c**) based on GC-MS metabolites of various *T. indica* organs as identified in Table 1.

Regarding TIF and TIS, γ-Sitosterol and n-Docosanoic acid were the chef compounds responsible for their separation in separate quadrants. By applying HCA, the dendrogram (Figure 3c) categorised *T. indica* organs into four main clusters. Cluster I, II, III, and IV displayed TIL, TIB, TIF, and TIS, respectively. The dendrogram showed that TIL and TIB were closely related to each other's when compared to TIF and TIS. Both PCA and HCA successfully discriminated among various *T. indica* organs proving the effective application of chemometric analysis in combination with GC/MS-based metabolites for the discrimination among various plant organs.

2.3. Anti-Inflammatory Activity of Tamarindus indica L. Various Organs

The anti-inflammatory effects of the *n*-hexane extract of *T. indica* bark, leaves, seeds, and fruits (TIB, TIL, TIS, and TIF) on lipopolysaccharide (LPS)-induced RAW 264.7 macrophages were represented in (Table 2). The various organs of *T. indica* showed promising inhibition of LPS-induced nitric oxide (NO) release in RAW 264.7 macrophages. At a concentration of 10 μg/mL, TIB, TIL, TIS, and TIF *n*-hexane extracts showed %NO inhibition by 7.53 ± 1.69, 53.97 ± 5.89, 19.54 ± 1.19, and $26.66 \pm 3.44\%$, respectively. Further, at a concentration of 100 μg/mL, TIB, TIL, TIS, and TIF *n*-hexane extracts showed %NO inhibition by 51.44 ± 1.17, 98.00 ± 1.90, 85.47 ± 0.22, and $83.69 \pm 2.39\%$, respectively as compared to positive control L-N^G-nitro arginine methyl ester (L-NAME) (1 mM) that showed $84.64 \pm 1.04\%$ NO inhibition.

Table 2. The anti-inflammatory effects of the *n*-hexane extract from various organs of *T. indica*: TIB (bark), TIL (leaves), TIS (seeds), and TIF (fruits) on lipopolysaccharide (LPS)-induced RAW 264.7 macrophages.

Sample	%NO Inhibition	
	10 μg/mL	**100 μg/mL**
TIB	7.53 ± 1.69 [b]	51.44 ± 1.17 [b]
TIL	53.97 ± 5.89 [b]	98.00 ± 1.90 [b]
TIS	19.54 ± 1.19 [b]	85.47 ± 0.22 [a]
TIF	26.66 ± 3.44 [b]	83.69 ± 2.39 [a]
L-NAME (1 mM)	84.64 ± 1.04 [a]	

Means bearing same scripts ([a] or [b]) are not significantly different from control at $p < 0.05$, Mean $\pm$ Standard error.

Previous studies revealed that the fruit pulp was applied to inflammations and traditionally used as a gargle for sore throats. Further, the bark decoction was used in cases of eye inflammation [12]. Rimbau et al. revealed the in vivo anti-inflammatory properties of different extracts of tamarind fruit pulp in mice ear oedema induced by arachidonic acid, and rats sub plantar oedema induced by carrageenan [43]. Moreover, the petroleum ether and ethyl acetate extracts of seeds of *T. indica* showed a significant anti-inflammatory and analgesic potential using carrageenan-induced paw oedema and cotton pellet-induced granuloma models in rats [44]. Among the major compounds in the *n*-hexane extract of *T. indica's* various organs were lupenone and sitosterol, which were reported for their anti-inflammatory activity [45]. Additionally, among the major identified compounds, lupeol and lupeol acetate were reported for their anti-inflammatory properties through regulating TNF-α, IL-2, and IL-β specific mRNA, reducing PGE-2 synthesis from macrophage, neutrophil migration, and the number of iNOS cells [46].

2.4. Wound Healing Activity of Tamarindus indica L. Various Organs

2.4.1. Cytotoxicity Assay

Evaluation of the cytotoxicity of the *n*-hexane extract of *T. indica* bark, leaves, seeds, and fruits (TIB, TIL, TIS, and TIL) on the HSF cells was necessary to assess the safety of the treatment dose. The cytotoxicity on HSF cells of the *n*-hexane extract of *T. indica's* various organs was evaluated using the SRB assay [47]. In our investigation, TIF and TIS (up to 100 μg/mL) had no cytotoxic effect on the HSF cells. While TIB and TIL at a

concentration of 10 μg/mL showed HSF cell viability up to 91.04 ± 2.09 and 95.38 ± 0.86%, respectively (Figure 4). Therefore, a concentration of 10 μg/mL was safe and used further as the treatment dose in the scratch wound assay.
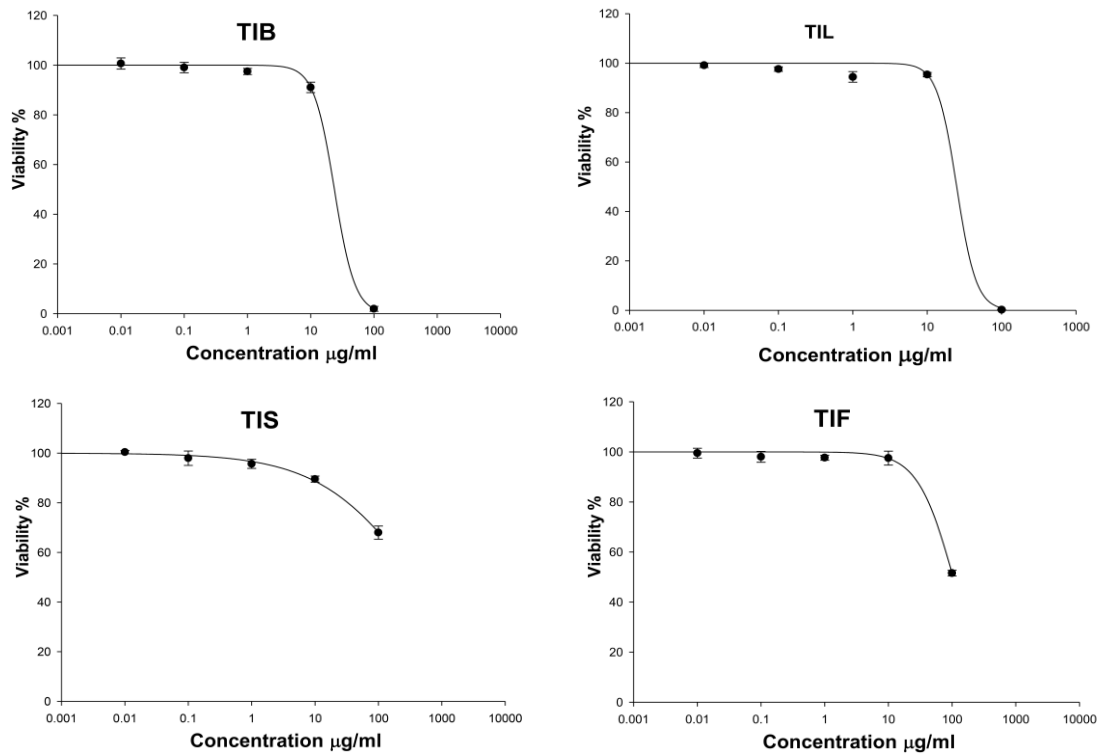

Figure 4. The effect of *n*-hexane extract from various organs of *T. indica*: TIB (bark), TIL (leaves), TIS (seeds), and TIF (fruits) on Human Skin Fibroblast cells (HSF) viability.

2.4.2. Scratch Wound Assay

In the present study, an in vitro scratch assay using HSF cells was used to assess TIB, TIL, TIS and TIF wound-healing activity. It was evaluated by changes in wound width by measuring the average distance between the borders of the scratches (Figures 5 and 6). The tested plant extracts at a concentration of 10 μg/mL decreased the wound width significantly compared with the control cells (Table 3).

Table 3. Wound width of the scratched Human Skin Fibroblast cells (HSF) incubated in the absence of the plant extract (negative control) and the presence of *n*-hexane extract from *T. indica*: TIB (bark), TIL (leaves), TIS (seeds), and TIF (fruits) (10 μg/mL).

Time (h)	Wound Width (mm)				
	TIB (10 μg/mL)	TIL (10 μg/mL)	TIS (10 μg/mL)	TIF (10 μg/mL)	Control
0	2.68 ± 0.02 [a]	2.75 ± 0.02 [a]	2.72 ± 0 [a]	2.74 ± 0.04 [a]	2.73 ± 0.03 [a]
24	1.09 ± 0.04 [a]	1.12 ± 0.18 [a]	1.09 ± 0.28 [a]	1.41 ± 0.35 [a]	1.37 ± 0.15 [a]
48	0 [a]	0.09 ± 0.16 [a]	0.13 ± 0.12 [a]	0.27 ± 0.12 [a]	0 [a]
72	0	0	0	0	0

Means bearing same script ([a]) are not significantly different from control at $p < 0.05$, Mean ± Standard error.
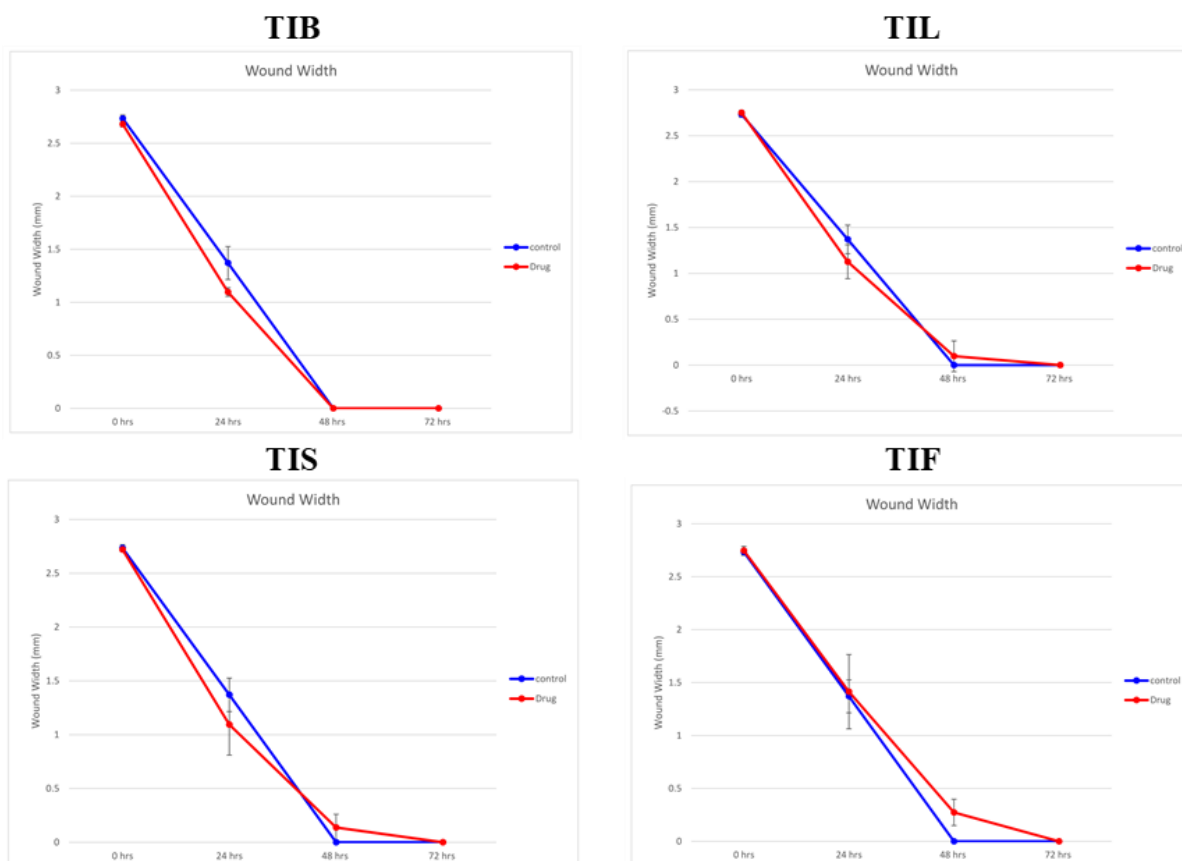
Figure 5. The wound width changes in the absence or presence of 10 μg/mL of *n*-hexane extract from various organs of *T. indica*: TIB (bark), TIL (leaves), TIS (seeds), and TIF (fruits).

After 24 h, the highest wound healing potential was recorded by TIB and TIS *n*-hexane extracts with wound widths equal to 1.09 ± 0.04 and 1.09 ± 0.28 mm, respectively. This result was followed by TIL and TIF with wound widths equal to 1.12 ± 0.18 and 1.41 ± 0.35 mm, respectively, as compared to the wound width in the control cells that equalled 1.37 ± 0.15 mm. As the wound width reduced as cell migration was enhanced, our findings revealed that both TIB and TIL *n*-hexane extracts exhibited almost complete cell migration after 48 h of observation. Meanwhile, TIS and TIF *n*-hexane extracts had wound-healing effects on HSF cells, but the time required to conduct wound closure was longer than for the negative control. This revealed that the *n*-hexane extract of *T. indica's* various organs exhibited wound-healing potential through fibroblast migration enhancement.

Previous reports revealed the traditional utilisation of tamarind in eye surgery for conjunctival cell adhesion and corneal wound healing [12]. In a study by Adeniyi et al., the wound-healing activity of *T. indica* leaves and pulp was investigated in the African catfish, and the results revealed the enhancement of the wound healing significantly in the fish-fed tamarind-fortified diets as a consequence of the elevation of antioxidant enzymes [48]. Attah et al. investigated the wound-healing potential of *T. indica* fruit paste in adult rabbits, and the results revealed wound closure acceleration and increasing epithelial migration and re-epithelialisation [49].
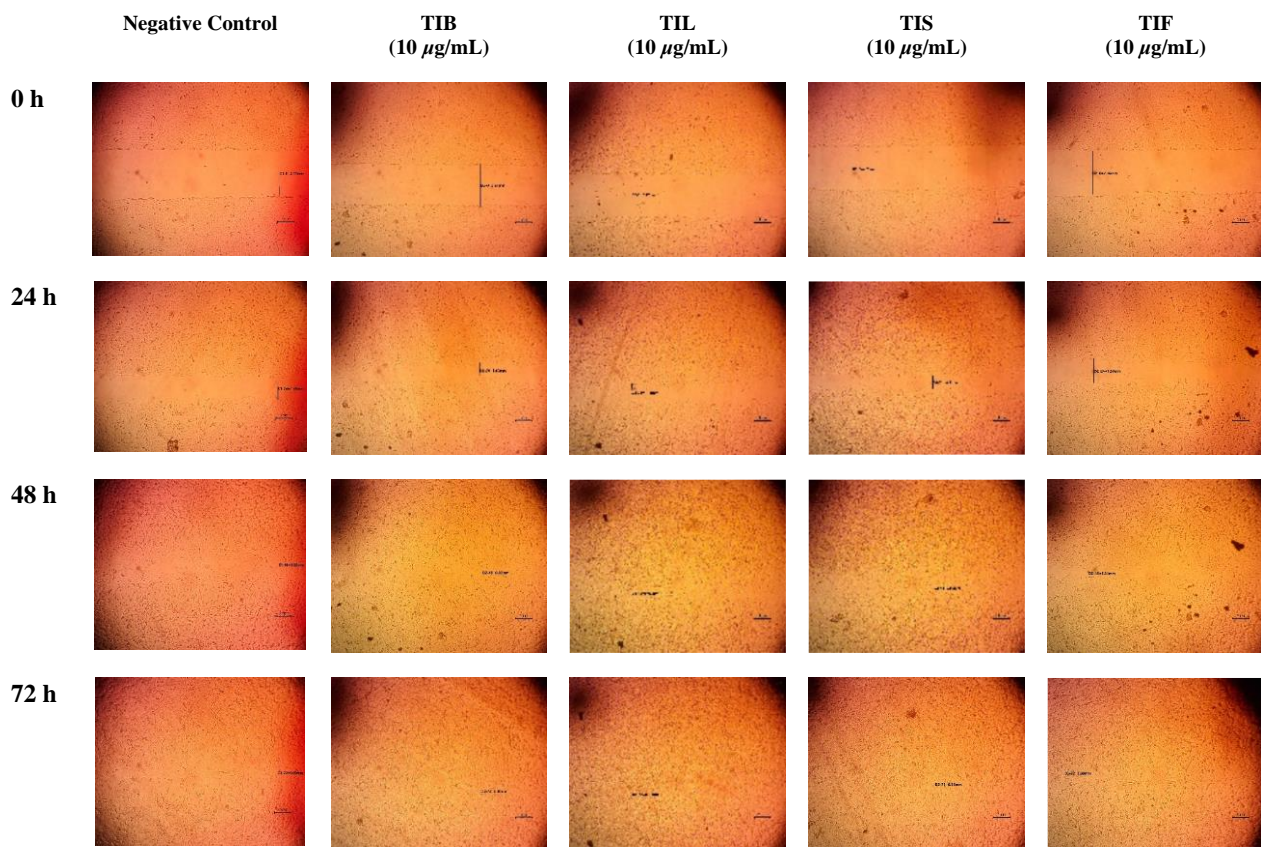
Figure 6. Microscopic images of (HSF) incubated in absence of the plant extract (negative control) and depicting the influence of 10 µg/mL of *n*-hexane extract from various organs of *T. indica*: TIB (bark), TIL (leaves), TIS (seeds), and TIF (fruits). Images were captured at 0, 24, 48 and 72 h. The boundaries of the scratched wounds are marked by dark lines.

The wound-healing potential of *n*-hexane extracts of various organs of *T. indica* can be linked to their chemical components. For example, γ-sitosterol is one of the most famous phytosterols with reported biological activity. Phytosterols were shown to inhibit MMP-1, reduce collagen breakdown, and promote the synthesis of collagen in human keratinocytes [50]. Moreover, they promote keratinocyte migration through the reduction of oxidative stress that effectively accelerates the healing process [51]. In previous studies, lupeol and lupeol acetate, which are the major identified components in the present study, were reported for their wound-healing properties [52–58]. Lupeol prevents collagen I depletion and restores levels of hydroxyproline, hexosamine, hexuronic acid, and matrix glycosaminoglycans, together with modulating collagen I expression in human fibroblasts during the proliferation phase. Further, it enhances fibroblast proliferation, angiogenesis, and growth factors in wound healing [52–54]. Another study reported the potential of lupeol for wound healing in streptozotocin-induced hyperglycaemic rats [56]. Another study by Malinowska et al. revealed that lupeol acetate was one of the most effective lupeol derivatives in the stimulation of the human skin cell proliferation process [58]. Bopage et al. reported that the presence of a 3-OH group in the lupeol structure is one of the essential features in the lupane skeleton for wound healing activity as compared to lupenone and lupeol acetate [59].

Linolenic acid and squalene are among the major identified constituents in the *n*-hexane extract of *T. indica* fruits; linolenic acid plays an important role in the wound healing process across its antioxidative and anti-inflammatory properties as well as by encouraging cell proliferation, raising collagen synthesis, promoting dermal reconstruction, and restoring the function of the skin's lipid barrier [60–63]. Further, squalene is reported to have anti-inflammatory and protective actions against skin damage. It can accelerate

the healing of wounds by stimulating the macrophage response to inflammation. Squalene could be helpful during the resolution phase of wound healing [64].

The amounts of lupeol, lupeol acetate, lupenone, and γ-sitosterol show a correlation with the in vitro wound healing potential of the *n*-hexane extract of various organs of *T. indica*, and TIB was found to contain the highest amounts of these compounds according to the GC/MS analysis. The present study and the data in the literature show that terpenoids, sterols, and fatty acids play important roles in the wound-healing potential of *T. indica*. So, *T. indica* is suggested as a potent natural wound-healing product.

2.5. In Silico Molecular Docking Studies

This part was conducted to investigate the possible mechanism of action in which the identified major compounds exert their biological effect. Accordingly, the 3D structures of glycogen synthase kinase 3-β (GSK3-β), matrix metalloproteinases-8 (MMP-8), and nitric oxide synthase (iNOS) were downloaded from the protein data bank using the following IDs: 3F88, 5H8X, and 3N2R, respectively. After that, the twenty major compounds were docked into the active site vicinity of the three enzymes. Interestingly, all the compounds achieved acceptable binding scores upon docking with the three targets (Table 4).

Table 4. The docking scores achieved by the major identified compounds against the three enzymes.

Compound Name	Docking Scores (Kcal/mol)		
	Glycogen Synthase Kinase 3-β (GSK3-β) 3F88	Nitric Oxide Reductase (iNOS) 3N2R	Matrix Metalloproteinases 8 (MMP-8) 5H8X
Lupeol	−12.5	−13.7	−9.8
n-docosanoic acid	−11.7	−12.6	−11.9
methyl tricosanoate	−11.2	−11.8	−13.1
α-terpinyl acetate	−11.8	−10.1	−12.5
α-muurolene	−10.4	−11.8	−10.1
Gamma- sitosterol	−10.2	−11.9	−8.2
Lupenone	−10.1	−10.3	−7.6
Lupeol acetate	−11.3	−9.5	−7.7
n-tetratriacontane	−9.8	−7.6	−7.5
Betulinaldehyde	−8.7	−8.1	−7.4
β-Amyrone	−9.2	−6.5	−7.1
24-methylenecycloartanol	−8.3	−7.2	−6.8
methyl tricosanoate	−7.8	−7.4	−7.5
n-hexacosane	−8.2	−7.8	−7.3
cis-13,16-docasadienoic acid	−7.5	−8.3	−6.5
n-tetratriacontane	−7.9	−9.1	−5.9
methyl pentadecanoate	−7.3	−7.8	−7.6
Squalene	−6.8	−7.8	−7.2
Linolenic acid	−8.1	−8.5	−7.9
n- pentacosane	−7.3	−7.7	−7.4

To this end, it was expected that the identified major compounds would exert synergetic effects. In the docking of GSK3-β-lupeol, n-docosanoic acid, methyl tricosanoate, α-terpinyl acetate, and lupeol acetate achieved best docking scores of −12.5, −11.7, −11.2, −11.8, and −11.3 Kcal/Mol, respectively. As Figure 7 reveals, lupeol interacted with Val135, Tyr140, Arg141, Gln185, and Cys199; n-docosanoic acid interacted with Gly63, Lys183, and Cys199; methyl tricosanoate interacted with GSK3-β through binding with Phe67, Arg141, and Cys199; α-terpinyl acetate interacted with Lys85, Asp133, and Cys199; and lupeol acetate interacted with Lys85, Gln185, and Cys199. In the docking of matrix metalloproteinases-8 (MMP-8), lupeol, n-docosanoic acid, methyl tricosanoate, α-terpinyl acetate, and α-muurolene achieved the best docking scores of −9.8, −11.9, −13.1, −12.5, and −10.1 Kcal/Mol, respectively. As depicted in Figure 8, lupeol bound to MMP-8 through

interactions with Ala161, Gly158, and Asn218; n-docosanoic acid interacted with Ala161, Glu198, His207, Pro217, and Asn218; methyl tricosanoate interacted with Asn85, Ala161, Ala163, Gln165, His 197, Glu198, His201, and Pro217; α-terpinyl acetate interacted with Ala161, Val194, His 197, Glu198, His207, Pro217, and Asn218; and α-muurolene interacted with MMP-8 through binding with His197, Leu214, and Tyr216. In the docking of Nitric oxide reductase (iNOS), lupeol, n-docosanoic acid, methyl tricosanoate, α-muurolene, and gamma-sitosterol achieved the best docking scores of −13.7, −12.6, −11.8, −11.8, and −11.9 Kcal/Mol, respectively. Looking at Figure 9, we see that lupeol was able to interact with the residues of iNOS through binding with Gln478, Tyr588, Glu592, Asp597, Trp678, and Val680; n-docosanoic acid interacted with Thr324, Arg414, Cys415, Gln478, Glu592, Trp678, and Asn697; methyl tricosanoate interacted with Trp409, Arg414, Cys415, Gly417, Met570, Phe584, and Glu592; α-muurolene interacted with Met336, Trp678, and Val680; and gamma-sitosterol interacted with Cys415, Val677, and Trp678. In conclusion, the docking results supported and justified the biological results giving rise to a synergetic effect for all the major components of the extract.
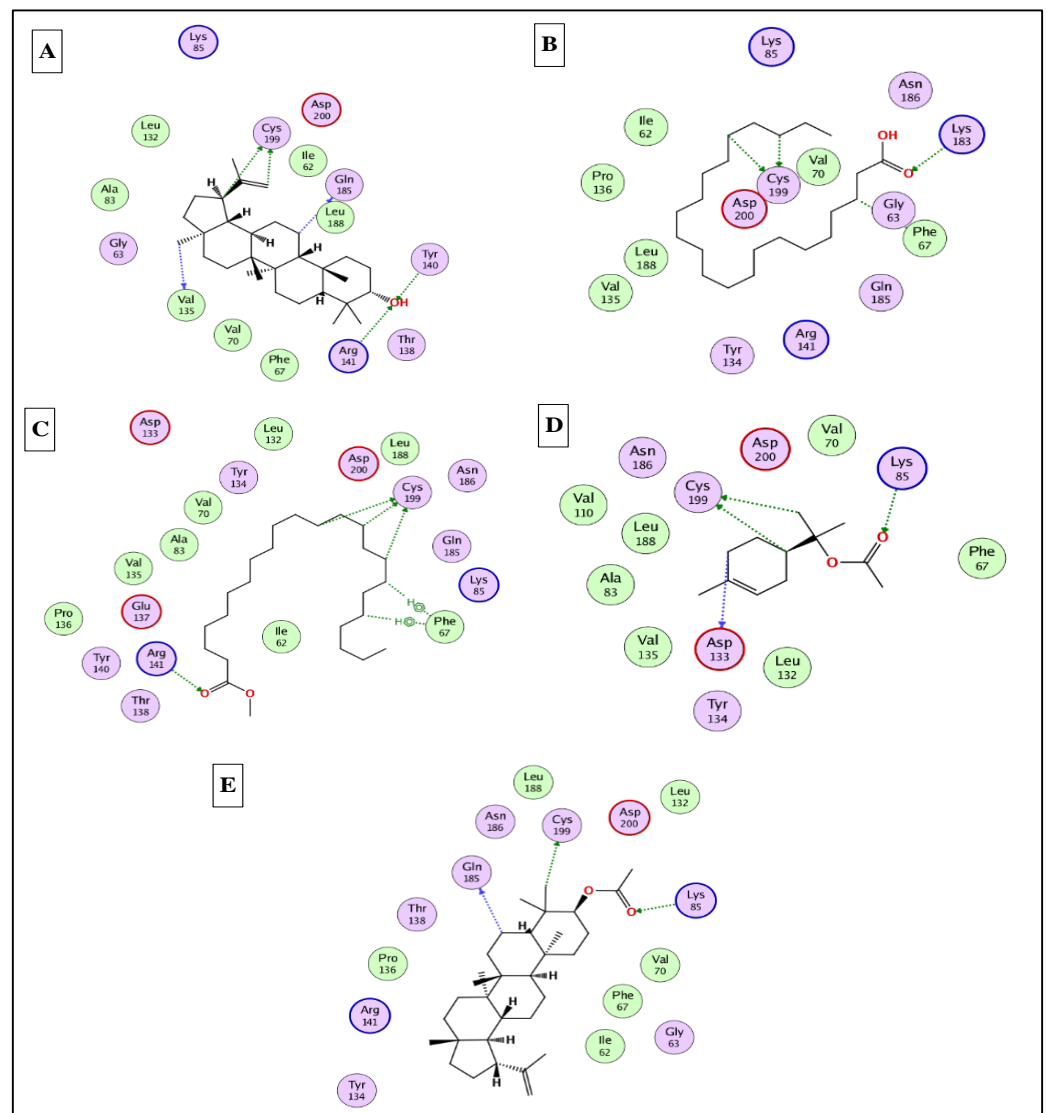
Figure 7. 2D binding modes of lupeol (**A**), n- docosanoic acid (**B**), methyl tricosanoate (**C**), α-terpinyl acetate (**D**), and lupeol acetate (**E**) to the active binding sites of glycogen synthase kinase 3-β (GSK3-β).
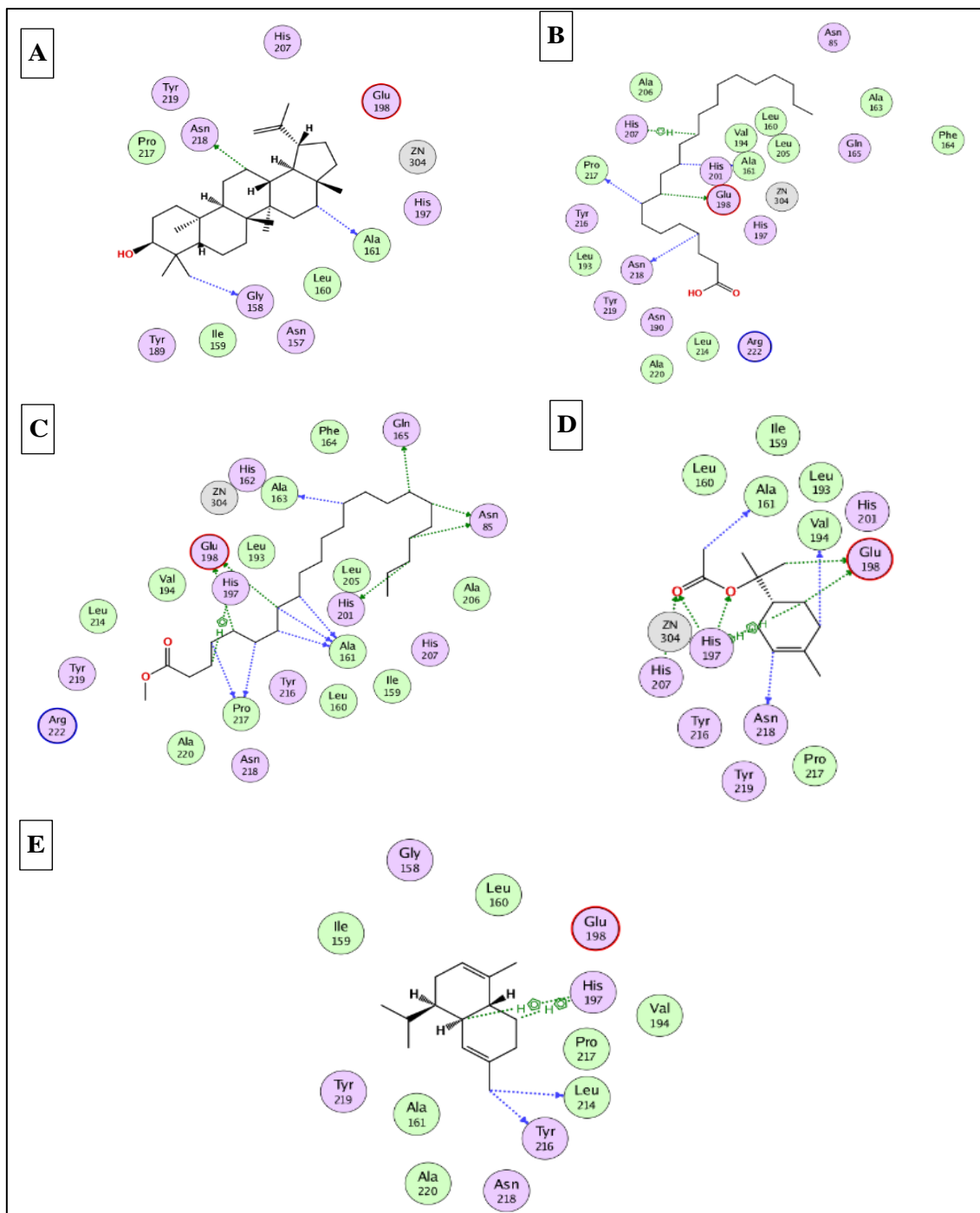
Figure 8. 2D binding modes of lupeol (**A**), n- docosanoic acid (**B**), methyl tricosanoate (**C**), α-terpinyl acetate (**D**), and α-muurolene (**E**) to the active binding sites of matrix metalloproteinases-8 (MMP-8).
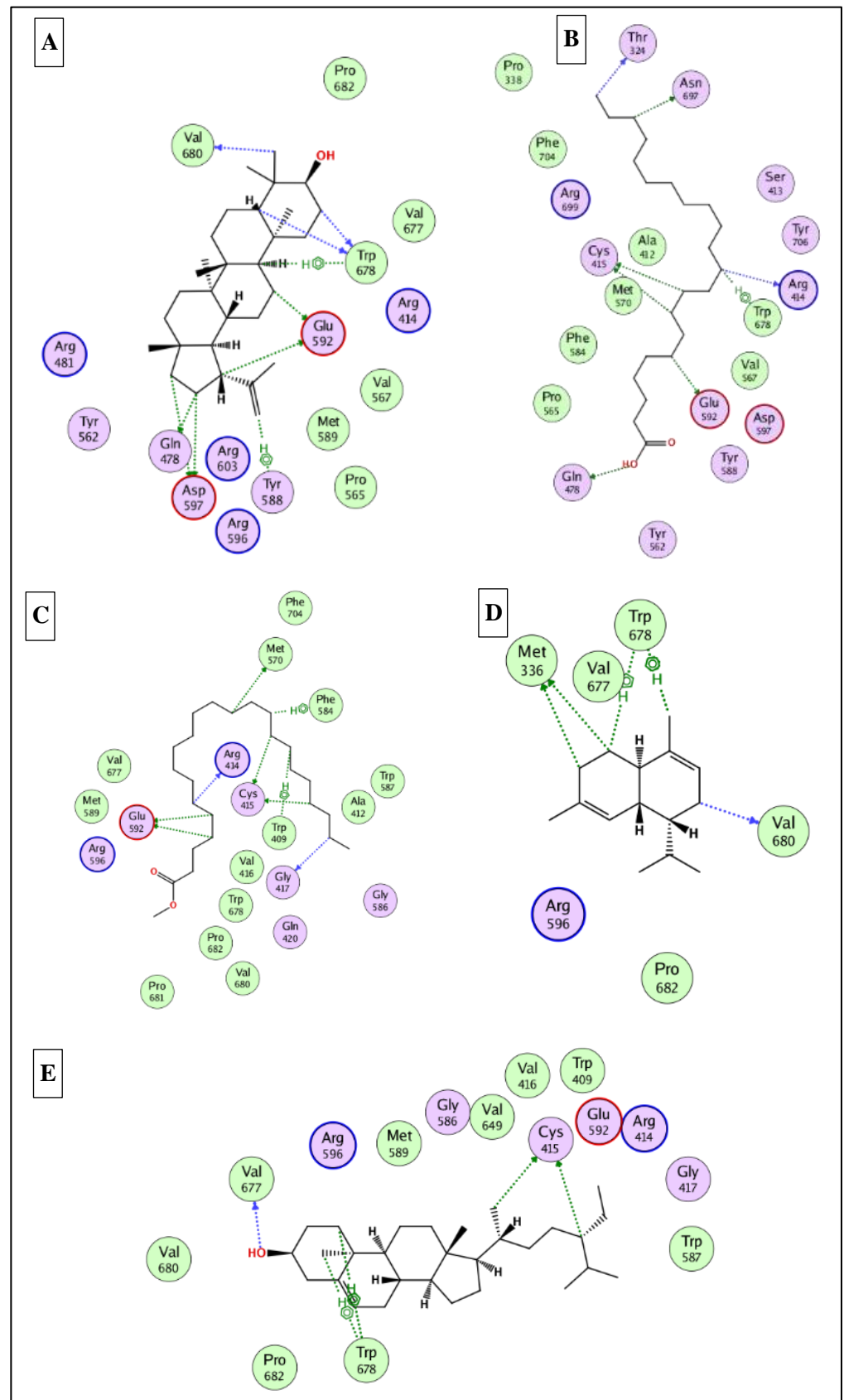
Figure 9. 2D binding modes of (**A**), n- docosanoic acid (**B**), methyl tricosanoate (**C**), α-muurolene (**D**), and gamma-sitosterol (**E**) to the active binding sites of nitric oxide synthase (iNOS).

3. Materials and Methods

3.1. Plant Material

Tamarindus indica L.'s (Fabaceae) various organs (Bark, leaves, seeds, and fruits) were collected from the Zoo Botanical Garden, Giza, Egypt, in October 2021. The various plant organs were kindly identified and authenticated by agricultural engineer Eng. Terase Labib, Consultant of Plant Taxonomy at the Ministry of Agriculture and El-Orman Botanical Garden, Giza, Egypt. Voucher specimens of the various plant organs with codes BUC-PHG-TIL-6, BUC- PHG-TIS-7, BUC- PHG-TIF-8, and BUC-PHG-TIB-9 were kept at the Department of Pharmacognosy, Badr University in Cairo, Cairo, Egypt.

3.2. Preparation of the N-Hexane Extracts of Various Organs

The dried samples of the barks, leaves, seeds, and fruits of *T. indica* (100 g each) were powdered and extracted by cold maceration method with *n*-hexane (500 mL × 3) separately, followed by filtration for 3 days. The filtrate of each plant material was completely evaporated *in vacuo* at 45 °C until dry to obtain the dried residue of the *n*-hexane extract (420 mg, 610 mg, 207 mg, and 312 mg) for barks, leaves, seeds, and fruits, respectively. The dried residue of each plant part was named as follows; *T. indica* bark (TIB), *T. indica* leaves (TIL), *T. indica* seeds (TIS), and *T. indica* fruits (TIF). All extracts were stored in a tight container at 4 °C in the refrigerator for further analysis [65].

3.3. GC/MS Analysis

Gas chromatography coupled with mass spectrometry (GC/MS) analyses were performed on a Shimadzu GCMS-QP 2010 (Shimadzu Corporation, Koyoto, Japan), provided using an Rtx-5MS (30 m × 0.25 mm i.d. × 0.25 μm film thickness) capillary column (Restek, Bellefonte, PA, USA) and attached to a Shimadzu mass spectrometer. The column temperature was initially set at 50 °C for 3 min. Then, the temperature was gradually increased from 50 to 300 °C at a rate of 5 °C/min and then isothermally maintained at 300 °C for 10 min. The temperature of the injector was kept at 280 °C. Helium was used as a carrier gas at a flow rate of 1.37 mL/min. The ion source and the interface were at temperatures of 280 and 220 °C, respectively. An injection of 1 μL of 1% *v/v* of diluted sample was achieved via a split mode adopting a split ratio of 15:1. Recording of the mass spectrum was performed in EI mode of 70 eV from m/z 35 to 500. Compound quantitation was performed based on the normalisation method, employing the reading of three chromatographic runs.

3.4. Identification of the N-Hexane Extract Components

The components of the *n*-hexane extracts were characterised by comparing their GC/MS spectra, fragmentation patterns, and retention indices with those reported in the literature data [66–72]. The retention indices were calculated relative to a homologous series of *n*-alkanes (C8–C28) injected under the same conditions.

3.5. Chemometric Analysis

The data obtained from GC-MS were subjected to multivariate analysis. Principal component analysis (PCA) was performed as the first step in data analysis to provide an overview of all observations and samples and to identify and evaluate groupings, trends, and strong outliers [73]. Hierarchal cluster analysis (HCA) was used to allow the clustering of samples. The clustering patterns were constructed by applying the complete linkage method. This presentation was more efficient when the distance between samples (points) was computed using the Euclidean method. Both PCA and HCA were achieved by utilising Unscrambler®X 10.4 from CAMO (Computer Aided Modeling, Viken, Norway) [74].

3.6. Anti-Inflammatory Activity

Murine macrophage RAW264.7 cells (ATCC®) were maintained in a complete Dulbecco's Modified Eagle's Medium (DMEM, Corning, NY, USA) supplemented with 10% foetal bovine serum, penicillin (100 U/mL), streptomycin sulphate (100 μg/mL), and 2 mM

L-glutamine in a humidified 5% CO_2 incubator. For passaging and treatment, cells were washed with phosphate-buffered saline and scrapped off the flasks using sterile scrappers (SPL, Spain). RAW 264.7 cell stock (0.5 × 106 cells/mL) was seeded into 96-well microwell plates and incubated overnight. The next day, the non-induced triplicate wells received a medium with the sample vehicle (DMSO, 0.1% *v/v*). The inflammation group of triplicate wells received the inducer of inflammation [lipopolysaccharide (LPS) as 100 ng/mL] in complete culture media containing 0.1% DMSO, *v/v*. Sample groups of triplicate wells received two screening amounts (10 and 50 μg/mL) of the sample dissolved in DMSO and diluted into culture media containing LPS (Final concentration of DMSO = 0.1%, by volume). L-NAME (L-N^G-nitro arginine methyl ester) (1 mM) was used as a standard NOS inhibitor. After 24 h of incubation, a Griess assay [75] was used to determine NO in all wells. Equal volumes of culture supernatants and Griess reagent were mixed and incubated at room temperature for 10 min to form the coloured diazonium salt and read at an absorbance of 520 nm. The NO Inhibition % of the test extract was calculated relative to the LPS-induced inflammation group, normalised to cell viability determined with the Alamar Blue™ reduction assay [76].

3.7. Wound Healing Activity

3.7.1. Cytotoxicity Assay

The cytotoxicity of the tested plant extract against the HSF (Human Skin Fibroblast) cell line was assessed prior to the wound-healing assay using the sulforhodamine B assay (SRB) [47]. The HSF cell line was obtained from Nawah Scientific Inc. (Mokatam, Cairo, Egypt). Cells were maintained in a DMEM medium supplemented with 100 mg/mL of streptomycin, 100 units/mL of penicillin, and 10% of heat-inactivated foetal bovine serum in a humidified 5% (*v/v*) CO_2 atmosphere at 37 °C. Aliquots of 100 μL of cell suspension (5 × 10^3 cells) were placed in 96-well plates and incubated in a complete medium for 24 h. Cells were treated with another aliquot of 100 μL medium containing DRSE at various concentrations (0.01, 0.1, 1, 10, and 100 μg/mL). After 72 h of drug exposure, cells were fixed by replacing the medium with 150 μL of 10% TCA and incubated at 4 °C for 1 h. The TCA solution was removed, and the cells were washed five times with distilled water. Aliquots of 70 μL SRB solution (0.4% *w/v*) were added and incubated in a dark place at room temperature for 10 min. Plates were washed three times with 1% acetic acid and allowed to air-dry overnight. Then, 150 μL of TRIS (10 mM) was added to dissolve the protein-bound SRB stain; the absorbance was measured at 540 nm using a BMGLABTECH®-FLUO star Omega microplate reader (Ortenberg, Germany).

3.7.2. Scratch Wound Assay

The wound-healing activity of TIB, TIL, TIS, and TIF *n*-hexane extract was evaluated using in vitro cell migration studies on HSF cells. Cells were plated at a density of 2 × 10^5/well onto a coated 12-well plate for the scratch wound assay and cultured overnight in 5% FBS-DMEM at 37 °C and 5% CO_2. On the next day, horizontal scratches were introduced into the confluent monolayer; the plate was washed thoroughly with PBS, control wells were replenished with the fresh medium, and drug wells were treated with fresh media containing the drug. Images were taken using an inverted microscope at the indicated time intervals. The plate was incubated at 37 °C and 5% CO_2 between time points. The experiment was done in triplicate. The acquired images are displayed in Figure 6 and were analysed using MII ImageView software version 3.7. Wound width was calculated as the average distance between the edges of the scratches; the wound width decreases as cell migration is induced. The results are displayed as mean ± standard deviation (Table 3) [77–79].

3.8. Statistical Analysis

Statistical analyses were done using a one-way analysis of variance (ANOVA) followed by the Tukey–Kramer multiple comparison test ($p < 0.05$). Statistical analyses were performed using GraphPad Prism 6.01 (GraphPad Inc., La Jolla, CA, USA).

3.9. In Silico Molecular Docking Studies

The X-ray 3D structures of glycogen synthase kinase 3-β (GSK3-β), matrix metalloproteinases-8 (MMP-8), and nitric oxide synthase (iNOS) were downloaded from the protein data bank www.pdb.org (accessed on 15 August 2022) using the following IDs: 3F88, 5H8X, and 3N2R, respectively [80–82]. All the docking studies were conducted using MOE 2019 [83], which was also used to generate the 2D interaction diagrams between the docked ligands and their potential targets. The identified major compounds were prepared using the default parameters and saved in a single MDB file. The active site for each target was determined from the binding of the corresponding co-crystalised ligand. Finally, the docking was finalised by docking the MDB file containing all the major compounds into the active site of the three enzymes.

4. Conclusions

The present study investigated the secondary metabolites in the *n*-hexane extract of *T. indica's* various organs and their in vitro anti-inflammatory and wound healing properties using the scratch assay with HSF cells. The GC/MS analysis revealed that triterpenoids and steroids were the predominant classes in the *T. indica* bark and leaf n-hexane extracts. Additionally, the seed and fruit *n*-hexane extracts showed a high percentage of fatty acids and higher hydrocarbons. PCA and HCA successfully discriminated various *T. indica* organs based on their GC/MS metabolites. The tested extracts showed promising anti-inflammatory and wound-healing properties. Additionally, the major characterised phytoconstituents achieved promising docking scores in the active sites of glycogen synthase kinase 3-β (GSK3-β), matrix metalloproteinases-8 (MMP-8), and nitric oxide synthase (iNOS), which give the *n*-hexane extract of the various *T. indica* organs a chance to be incorporated in the pharmaceutical products for wound healing after further in vivo and clinical trials.

References

1. Elmaidomy, A.H.; Abdelmohsen, U.R.; Alsenani, F.; Aly, H.F.; Shams, S.G.E.; Younis, E.A.; Ahmed, K.A.; Sayed, A.M.; Owis, A.I.; Afifi, N.; et al. The Anti-Alzheimer Potential of Tamarindus Indica: An in Vivo Investigation Supported by in Vitro and in Silico Approaches. *RSC Adv.* **2022**, *12*, 11769–11785. [CrossRef] [PubMed]
2. Chong, U.R.W.; Abdul-Rahman, P.S.; Abdul-Aziz, A.; Hashim, O.H.; Mat Junit, S. *Tamarindus indica* Extract Alters Release of Alpha Enolase, Apolipoprotein A-I, Transthyretin and Rab GDP Dissociation Inhibitor Beta from HepG2 Cells. *PLoS ONE* **2012**, *7*, e39476. [CrossRef] [PubMed]
3. Havinga, R.M.; Hartl, A.; Putscher, J.; Prehsler, S.; Buchmann, C.; Vogl, C.R. *Tamarindus indica* L. (Fabaceae): Patterns of Use in Traditional African Medicine. *J. Ethnopharmacol.* **2010**, *127*, 573–588. [CrossRef] [PubMed]
4. Lim, C.Y.; Mat Junit, S.; Abdulla, M.A.; Abdul Aziz, A. In Vivo Biochemical and Gene Expression Analyses of the Antioxidant Activities and Hypocholesterolaemic Properties of *Tamarindus indica* Fruit Pulp Extract. *PLoS ONE* **2013**, *8*, e70058. [CrossRef]
5. Aly, S.H.; Elissawy, A.M.; Eldahshan, O.A.; Elshanawany, M.A.; Efferth, T.; Singab, A.N.B. The Pharmacology of the Genus *Sophora* (Fabaceae): An Updated Review. *Phytomedicine* **2019**, *64*, 153070. [CrossRef] [PubMed]
6. Eldahshan, O.; Aly, S.; Elissawy, A.; Elshanawany, M.; Singab, A.N. Morphological and Genetic Characteristics of *Sophora secundiflora* and *Sophora tomentosa* (Fabaceae) Cultivated in Egypt. *Taeckholmia* **2019**, *39*, 103–129. [CrossRef]
7. Abdelrahman, G.H.; Mariod, A.A. *Wild Fruits: Composition, Nutritional Value and Products*; Springer: Berlin/Heidelberg, Germany, 2019; ISBN 9783030318857.
8. Kuru, P. Tamarindus Indica and Its Health Related Effects. *Asian Pac. J. Trop. Biomed.* **2014**, *4*, 676–681. [CrossRef]
9. Martinello, F.; Soares, S.M.; Franco, J.J.; Santos, A.C.; Sugohara, A.; Garcia, S.B.; Curti, C.; Uyemura, S.A. Hypolipemic and Antioxidant Activities from *Tamarindus indica* L. Pulp Fruit Extract in Hypercholesterolemic Hamsters. *Food Chem. Toxicol. Int. J. Publ. Br. Ind. Biol. Res. Assoc.* **2006**, *44*, 810–818. [CrossRef] [PubMed]
10. Bhadoriya, S.S.; Mishra, V.; Raut, S.; Ganeshpurkar, A.; Jain, S.K. Anti-Inflammatory and Antinociceptive Activities of a Hydroethanolic Extract of *Tamarindus indica* Leaves. *Sci. Pharm.* **2012**, *80*, 685–700. [CrossRef]
11. Maiti, R.; Jana, D.; Das, U.K.; Ghosh, D. Antidiabetic Effect of Aqueous Extract of Seed of *Tamarindus indica* in Streptozotocin-Induced Diabetic Rats. *J. Ethnopharmacol.* **2004**, *92*, 85–91. [CrossRef]
12. De Caluwé, E.; Halamová, K.; Van Damme, P. Tamarind (*Tamarindus indica* L.): A Review of Traditional Uses, Phytochemistry and Pharmacology. *ACS Symp. Ser.* **2009**, *1021*, 85–110. [CrossRef]
13. Naeem, N.; Nadeem, F.; Azeem, M.W.; Dharmadasa, R.M. *Tamarindus indica*—A Review of Explored Potentials. *Int. J. Chem. Biochem. Sci.* **2017**, *12*, 98–106.
14. Escalona-Arranz, J.; Péres-Roses, R.; Urdaneta-Laffita, I.; Camacho-Pozo, M.; Rodríguez-Amado, J.; Licea-Jiménez, I. Antimicrobial Activity of Extracts from *Tamarindus indica* L. Leaves. *Pharmacogn. Mag.* **2010**, *6*, 242–247. [CrossRef] [PubMed]
15. Al-Fatimi, M.; Wurster, M.; Schröder, G.; Lindequist, U. Antioxidant, Antimicrobial and Cytotoxic Activities of Selected Medicinal Plants from Yemen. *J. Ethnopharmacol.* **2007**, *111*, 657–666. [CrossRef] [PubMed]
16. Meléndez, P.A.; Capriles, V.A. Antibacterial Properties of Tropical Plants from Puerto Rico. *Phytomedicine* **2006**, *13*, 272–276. [CrossRef]
17. Komakech, R.; Kim, Y.; Matsabisa, G.M.; Kang, Y. Anti-Inflammatory and Analgesic Potential of *Tamarindus indica* Linn. (Fabaceae): A Narrative Review. *Integr. Med. Res.* **2019**, *8*, 181–186. [CrossRef]
18. Meher, B.; Dash, D.K.; Kumar Dash, D.; Roy, A. A Review on: Phytochemistry, Pharmacology and Traditional Uses of *Tamarindus indica* L. *World J. Pharm. Pharm. Sci.* **2014**, *3*, 229.
19. Yerima, M.; Anuka, J.A.; Salawu, O.A.; Abdu-Aguye, I. Antihyperglycaemic Activity of the Stem-Bark Extract of *Tamarindus indica* L. on Experimentally Induced Hyperglycaemic and Normoglycaemic Wistar Rats. *Pak. J. Biol. Sci. PJBS* **2014**, *17*, 414–418. [CrossRef]
20. Das, S.S.; Dey, M.; Ghosh, A.K. Determination of Anthelmintic Activity of the Leaf and Bark Extract of *Tamarindus indica* Linn. *Indian J. Pharm. Sci.* **2011**, *73*, 104–107. [CrossRef]
21. Okur, M.E.; Karadağ, A.E.; Okur, N.Ü.; Özhan, Y.; Sipahi, H.; Ayla, Ş.; Daylan, B.; Demirci, B.; Demirci, F. In Vivo Wound Healing and in Vitro Anti-Inflammatory Activity Evaluation of *Phlomis russeliana* Extract Gel Formulations. *Molecules* **2020**, *25*, 2695. [CrossRef]
22. Bakr, R.O.; Amer, R.I.; Attia, D.; Abdelhafez, M.M.; Al-Mokaddem, A.K.; El Gendy, A.N.; El-Fishawy, A.M.; Fayed, M.A.A.; Gad, S.S. In-Vivo Wound Healing Activity of a Novel Composite Sponge Loaded with Mucilage and Lipoidal Matter of Hibiscus Species. *Biomed. Pharmacother.* **2021**, *135*, 111225. [CrossRef] [PubMed]
23. Imran, M.; Sharma, J.N.; Kamal, M.; Asif, M. Standardization and Wound-Healing Activity of Petroleum, Ethanolic and Aqueous Extracts of *Ficus benghalensis* Leaves. *Pharm. Chem. J.* **2021**, *54*, 1057–1062. [CrossRef]
24. Agyare, C.; Boakye, Y.D.; Bekoe, E.O.; Hensel, A.; Dapaah, S.O.; Appiah, T. Review: African Medicinal Plants with Wound Healing Properties. *J. Ethnopharmacol.* **2016**, *177*, 85–100. [CrossRef] [PubMed]
25. Haque, S.D.; Saha, S.K.; Salma, U.; Nishi, M.K.; Rahaman, M.S. Antibacterial Effect of Aloe Vera (*Aloe barbadensis*) Leaf Gel against *Staphylococcus aureus*, *Pseudomonas aeruginosa*, *Escherichia coli* and *Klebsiella pneumoniae*. *Mymensingh Med. J.* **2019**, *28*, 490–496. [CrossRef] [PubMed]
26. Shedoeva, A.; Leavesley, D.; Upton, Z.; Fan, C. Wound Healing and the Use of Medicinal Plants. *Evid.-Based Complement. Altern. Med.* **2019**, *2019*, 2684108. [CrossRef] [PubMed]

27. Ads, E.N.; Hassan, S.I.; Rajendrasozhan, S.; Hetta, M.H.; Aly, S.H.; Ali, M.A. Isolation, Structure Elucidation and Antimicrobial Evaluation of Natural Pentacyclic Triterpenoids and Phytochemical Investigation of Different Fractions of *Ziziphus spina-christi* (L.) Stem Bark Using LCHRMS Analysis. *Molecules* **2022**, *27*, 1805. [CrossRef]

28. El-Nashar, H.A.S.; Aly, S.H.; Ahmadi, A.; El-Shazly, M. The Impact of Polyphenolics in the Management of Breast Cancer: Mechanistic Aspects and Recent Patents. *Recent Pat. Anticancer Drug Discov.* **2021**, *17*, 358–379. [CrossRef]

29. Aly, S.H.; Elgindi, M.R.; Singab, A.E.N.B.; Mahmoud, I.I. *Hyophorbe verschaffeltii* DNA Profiling, Chemical Composition of the Lipophilic Fraction, Antimicrobial, Anti-Inflammatory and Cytotoxic Activities. *Res. J. Pharm. Biol. Chem. Sci.* **2016**, *7*, 120–130.

30. Aly, S.H.; Elissawy, A.M.; Fayez, A.M.; Eldahshan, O.A.; Elshanawany, M.A.; Singab, A.N.B. Neuroprotective Effects of *Sophora secundiflora*, *Sophora tomentosa* Leaves and Formononetin on Scopolamine-Induced Dementia. *Nat. Prod. Res.* **2021**, *35*, 5848–5852. [CrossRef]

31. Saber, F.R.; Aly, S.H.; Khallaf, M.A.; El-Nashar, H.A.S.; Fahmy, N.M.; El-Shazly, M.; Radha, R.; Prakash, S.; Kumar, M.; Taha, D.; et al. *Hyphaene thebaica* (Areceaeae) as a Promising Functional Food: Extraction, Analytical Techniques, Bioactivity, Food, and Industrial Applications. *Food Anal. Methods* **2022**, 1–21. [CrossRef]

32. Raslan, M.A.; Afifi, A.H. In Vitro Wound Healing Properties, Antioxidant Activities, HPLC-ESI-MS/MS Profile and Phytoconstituents of the Stem Aqueous Methanolic Extract of *Dracaena reflexa* Lam. *Biomed. Chromatogr.* **2022**, *36*, e5352. [CrossRef] [PubMed]

33. Labib, R.M.; Ayoub, I.M.; Michel, H.E.; Mehanny, M.; Kamil, V.; Hany, M.; Magdy, M.; Moataz, A.; Maged, B.; Mohamed, A. Appraisal on the Wound Healing Potential of *Melaleuca alternifolia* and *Rosmarinus officinalis* L. Essential Oil-Loaded Chitosan Topical Preparations. *PLoS ONE* **2019**, *14*, e0219561. [CrossRef] [PubMed]

34. El-Nashar, H.A.S.; Mostafa, N.M.; Eldahshan, O.A.; Singab, A.N.B. Chemical Composition, Cytotoxic and Anti-Arthritic Activities of Hexane Extracts of Certain *Schinus* Species. *J. Pharm. Pharmacol.* **2021**, *9*, 378–386. [CrossRef]

35. Aly, S.H.; Eldahshan, O.A.; Al-Rashood, S.T.; Binjubair, F.A.; El-Hassab, M.A.; Eldehna, W.M.; Acqua, S.D.; Zengin, G. Chemical Constituents, Antioxidant, and Enzyme Inhibitory Activities Supported by In-Silico Study of n-Hexane Extract and Essential Oil of Guava Leaves. *Molecules* **2022**, *27*, 8979. [CrossRef]

36. Ali, A.; Garg, P.; Goyal, R.; Kaur, G.; Li, X.; Negi, P.; Valis, M.; Kuca, K.; Kulshrestha, S. A Novel Herbal Hydrogel Formulation of *Moringa oleifera* for Wound Healing. *Plants* **2020**, *10*, 25. [CrossRef]

37. Ayoub, I.M.; Korinek, M.; El-Shazly, M.; Wetterauer, B.; El-Beshbishy, H.A. Activity of *Chasmanthe aethiopica* Leaf Extract and Its Profiling Using LC/MS and GLC/MS. *Plants* **2021**, *10*, 1118. [CrossRef]

38. Sakib, S.A.; Tareq, A.M.; Islam, A.; Rakib, A.; Islam, M.N.; Uddin, M.A.; Rahman, M.M.; Seidel, V.; Emran, T. Bin Anti-Inflammatory, Thrombolytic and Hair-Growth Promoting Activity of the n-Hexane Fraction of the Methanol Extract of *Leea indica* Leaves. *Plants* **2021**, *10*, 1081. [CrossRef]

39. Carullo, G.; Sciubba, F.; Governa, P.; Mazzotta, S.; Frattaruolo, L.; Grillo, G.; Cappello, A.R.; Cravotto, G.; Di Cocco, M.E.; Aiello, F. Mantonico and Pecorello Grape Seed Extracts: Chemical Characterization and Evaluation of In Vitro Wound-Healing and Anti-Inflammatory Activities. *Pharmaceuticals* **2020**, *13*, 97. [CrossRef]

40. Ibrahim, N.A.; El-Gengaihi, S.; El-Hamidi, A.; Bashandy, S.A.E. Chemical and Biological Evaluation of *Tamarindus indica* L. Growing in Sudan. *Acta Hortic.* **1995**, *390*, 51–58. [CrossRef]

41. Carasek, E.; Pawliszyn, J. Screening of Tropical Fruit Volatile Compounds Using Solid-Phase Microextraction (SPME) Fibers and Internally Cooled SPME Fiber. *J. Agric. Food Chem.* **2006**, *54*, 8688–8696. [CrossRef]

42. Gad, H.A.; Mukhammadiev, E.A.; Zengen, G.; Musayeib, N.M.A.; Hussain, H.; Bin Ware, I.; Ashour, M.L.; Mamadalieva, N.Z. Chemometric Analysis Based on GC-MS Chemical Profiles of Three Stachys Species from Uzbekistan and Their Biological Activity. *Plants* **2022**, *11*, 1215. [CrossRef] [PubMed]

43. Rimbau, V.; Cerdan, C.; Vila, R.; Iglesias, J. Antiinflammatory Activity of Some Extracts from Plants Used in the Traditional Medicine of North-African Countries (II). *Phyther. Res.* **1999**, *13*, 128–132. [CrossRef]

44. Hivrale, M.G.; Bandawane, D.D.; Mali, A.A. Anti-Inflammatory and Analgesic Activities of Petroleum Ether and Ethyl Acetate Fractions of *Tamarindus indica* Seeds. *Orient. Pharm. Exp. Med.* **2013**, *13*, 319–326. [CrossRef]

45. Dias, A.M.A.; Rey-Rico, A.; Oliveira, R.A.; Marceneiro, S.; Alvarez-Lorenzo, C.; Concheiro, A.; Júnior, R.N.C.; Braga, M.E.M.; De Sousa, H.C. Wound Dressings Loaded with an Anti-Inflammatory Jucá (*Libidibia ferrea*) Extract Using Supercritical Carbon Dioxide Technology. *J. Supercrit. Fluids* **2013**, *74*, 34–45. [CrossRef]

46. Lucetti, D.L.; Lucetti, E.C.; Bandeira, M.A.M.; Veras, H.N.; Silva, A.H.; Leal, L.K.A.; Lopes, A.A.; Alves, V.C.; Silva, G.S.; Brito, G.A.; et al. Anti-Inflammatory Effects and Possible Mechanism of Action of Lupeol Acetate Isolated from *Himatanthus drasticus* (Mart.) Plumel. *J. Inflamm.* **2010**, *7*, 60. [CrossRef]

47. Skehan, P.; Storeng, R.; Scudiero, D.; Monks, A.; McMahon, J.; Vistica, D.; Warren, J.T.; Bokesch, H.; Kenney, S.; Boyd, M.R. New Colorimetric Cytotoxicity Assay for Anticancer—Drug Screening. *J. Natl. Cancer Inst.* **1990**, *82*, 1107–1112. [CrossRef]

48. Adeniyi, O.V.; Olaifa, F.E.; Emikpe, B.O.; Oyagbemi, A.A. Experimental Evaluation of the Wound-Healing and Antioxidant Activities of Tamarind (*Tamarindus indica*) Pulp and Leaf Meal in the African Catfish (*Clarias gariepinus*). *Acta Vet. Eurasia* **2018**, *44*, 63–72. [CrossRef]

49. Attah, M.O.; Ishaya, H.B.; Chiroma, M.S.; Amaza, D.; Balogun, S.U.; Jacks, T. Effect of *Tamarindus indica* (Linn) on the Rate of Wound Healing in Adult Rabbits. *IOSR J. Dent. Med. Sci.* **2015**, *14*, 2279–2861. [CrossRef]

50. Poljšak, N.; Kočevar Glavač, N. *Tilia* Sp. Seed Oil—Composition, Antioxidant Activity and Potential Use. *Appl. Sci.* **2021**, *11*, 4932. [CrossRef]

51. Hernandez, G.R.; Hernandez Garcia, D.Y.; Sanchez, M.L. Healing Cream *Tournefortia hirsutissima* L. *Med. Aromat. Plants* **2017**, *6*, 4–6. [CrossRef]

52. Hata, K.; Hori, K.; Takahashi, S. Role of P38 MAPK in Lupeol-Induced B16 2F2 Mouse Melanoma Cell Differentiation. *J. Biochem.* **2003**, *134*, 441–445. [CrossRef] [PubMed]

53. Geetha, T.; Varalakshmi, P. Anti-Inflammatory Activity of Lupeol and Lupeol Linoleate in Rats. *J. Ethnopharmacol.* **2001**, *76*, 77–80. [CrossRef] [PubMed]

54. Pereira Beserra, F.; Xue, M.; Maia, G.L.d.A.; Leite Rozza, A.; Helena Pellizzon, C.; Jackson, C.J. Lupeol, a Pentacyclic Triterpene, Promotes Migration, Wound Closure, and Contractile Effect In Vitro: Possible Involvement of PI3K/Akt and P38/ERK/MAPK Pathways. *Molecules* **2018**, *23*, 2819. [CrossRef] [PubMed]

55. Patel, S.; Srivastava, S.; Singh, M.R.; Singh, D. Preparation and Optimization of Chitosan-Gelatin Films for Sustained Delivery of Lupeol for Wound Healing. *Int. J. Biol. Macromol.* **2018**, *107*, 1888–1897. [CrossRef] [PubMed]

56. Beserra, F.P.; Vieira, A.J.; Gushiken, L.F.S.; De Souza, E.O.; Hussni, M.F.; Hussni, C.A.; Takahira, R.K.; Nóbrega, R.H.; Martinez, E.R.M.; Jackson, C.J.; et al. Lupeol, a Dietary Triterpene, Enhances Wound Healing in Streptozotocin-Induced Hyperglycemic Rats with Modulatory Effects on Inflammation, Oxidative Stress, and Angiogenesis. *Oxidative Med. Cell. Longev.* **2019**, *2019*, 3182627. [CrossRef] [PubMed]

57. Bopage, N.S.; Kamal Bandara Gunaherath, G.M.; Jayawardena, K.H.; Wijeyaratne, S.C.; Abeysekera, A.M.; Somaratne, S. Dual Function of Active Constituents from Bark of *Ficus Racemosa* L. in Wound Healing. *BMC Complement. Altern. Med.* **2018**, *18*, 29. [CrossRef] [PubMed]

58. Malinowska, M.; Miroslaw, B.; Sikora, E.; Ogonowski, J.; Wojtkiewicz, A.M.; Szaleniec, M.; Pasikowska-Piwko, M.; Eris, I. New Lupeol Esters as Active Substances in the Treatment of Skin Damage. *PLoS ONE* **2019**, *14*, e0214216. [CrossRef]

59. Bopage, N.S.; Jayawardena, K.H.; Wijeyaratne, C.; Abeysekera, A.M.; Gunaherath, G.M.K.B. Wound Healing Activity of Some Lupeol Derivatives Using. *Life Sci.* **2016**, 3–5.

60. Poljšak, N.; Kreft, S.; Kočevar Glavač, N. Vegetable Butters and Oils in Skin Wound Healing: Scientific Evidence for New Opportunities in Dermatology. *Phyther. Res.* **2020**, *34*, 254–269. [CrossRef]

61. Lewinska, A.; Zebrowski, J.; Duda, M.; Gorka, A.; Wnuk, M. Fatty Acid Profile and Biological Activities of Linseed and Rapeseed Oils. *Molecules* **2015**, *20*, 22872–22880. [CrossRef]

62. Xu, A.L.; Xue, Y.-Y.; Tao, W.-T.; Wang, S.-Q.; Xu, H.-Q. Oleanolic Acid Combined with Olaparib Enhances Radiosensitization in Triple Negative Breast Cancer and Hypoxia Imaging with (18)F-FETNIM Micro PET/CT. *Biomed. Pharmacother.* **2022**, *150*, 113007. [CrossRef] [PubMed]

63. Lin, T.-K.; Zhong, L.; Santiago, J.L. Anti-Inflammatory and Skin Barrier Repair Effects of Topical Application of Some Plant Oils. *Int. J. Mol. Sci.* **2017**, *19*, 70. [CrossRef] [PubMed]

64. Sánchez-Quesada, C.; López-Biedma, A.; Toledo, E.; Gaforio, J.J. Squalene Stimulates a Key Innate Immune Cell to Foster Wound Healing and Tissue Repair. *Evid.-Based Complement. Altern. Med.* **2018**, *2018*, 9473094. [CrossRef]

65. Abd El-Ghffar, E.A.; El-Nashar, H.A.S.; Eldahshan, O.A.; Singab, A.N.B. GC-MS Analysis and Hepatoprotective Activity of the n-Hexane Extract of *Acrocarpus fraxinifolius* Leaves against Paracetamol-Induced Hepatotoxicity in Male Albino Rats. *Pharm. Biol.* **2017**, *55*, 444–449. [CrossRef]

66. Rostad, C.E.; Pereira, W.E. Kovats and Lee Retention Indices Determined by Gas Chromatography/Mass Spectrometry for Organic Compounds of Environmental Interest. *J. High Resolut. Chromatogr.* **1986**, *9*, 328–334. [CrossRef]

67. Ivanov, I.; Dincheva, I.; Badjakov, I.; Petkova, N.; Denev, P.; Pavlov, A. GC-MS Analysis of Unpolar Fraction from *Ficus carica* L. (Fig) Leaves. *Int. Food Res. J.* **2018**, *25*, 282–286.

68. de Carvalho, F.M.d.A.; Schneider, J.K.; de Jesus, C.V.F.; de Andrade, L.N.; Amaral, R.G.; David, J.M.; Krause, L.C.; Severino, P.; Soares, C.M.F.; Bastos, E.C.; et al. Brazilian Red Propolis: Extracts Production, Physicochemical Characterization, and Cytotoxicity Profile for Antitumor Activity. *Biomolecules* **2020**, *10*, 726. [CrossRef]

69. El-Nashar, H.A.S.; Eldehna, W.M.; Al-Rashood, S.T.; Alharbi, A.; Eskandrani, R.O.; Aly, S.H. GC/MS Analysis of Essential Oil and Enzyme Inhibitory Activities of *Syzygium cumini* (Pamposia) Grown in Docking Studies. *Molecules* **2021**, *26*, 6984. [CrossRef]

70. Aly, S.H.; Elissawy, A.M.; Eldahshan, O.A.; Elshanawany, M.A.; Singab, A.N.B. Phytochemical Investigation Using GC/MS Analysis and Evaluation of Antimicrobial and Cytotoxic Activities of the Lipoidal Matter of Leaves of *Sophora secundiflora* and *Sophora tomentosa*. *Arch. Pharm. Sci. Ain Shams Univ.* **2020**, *4*, 207–214. [CrossRef]

71. Aly, S.H.; Elissawy, A.M.; Eldahshan, O.A.; Elshanawany, M.A.; Singab, A.N.B. Variability of the Chemical Composition of the Essential Oils of Flowers and the Alkaloid Contents of Leaves of *Sophora secundiflora* and *Sophora tomentosa*. *J. Essent. Oil-Bear. Plants* **2020**, *23*, 442–452. [CrossRef]

72. Gad, H.A.; Ayoub, I.M.; Wink, M. Phytochemical Profiling and Seasonal Variation of Essential Oils of Three *Callistemon* Species Cultivated in Egypt. *PLoS One* **2019**, *14*, e0219571. [CrossRef] [PubMed]

73. Gad, H.A.; Mamadalieva, R.Z.; Khalil, N.; Zengin, G.; Najar, B.; Khojimatov, O.K.; Al Musayeib, N.M.; Ashour, M.L.; Mamadalieva, N.Z. GC-MS Chemical Profiling, Biological Investigation of Three *Salvia* Species Growing in Uzbekistan. *Molecules* **2022**, *27*, 5365. [CrossRef] [PubMed]

74. Brereton, R.G. *Applied Chemometrics for Scientists*; John Wiley & Sons: Chichester, UK, 2007; pp. 1–379.

75. Yoo, M.-S.; Shin, J.-S.; Choi, H.-E.; Cho, Y.-W.; Bang, M.-H.; Baek, N.-I.; Lee, K.-T. Fucosterol Isolated from *Undaria pinnatifida* Inhibits Lipopolysaccharide-Induced Production of Nitric Oxide and Pro-Inflammatory Cytokines via the Inactivation of Nuclear Factor-ΚB and P38 Mitogen-Activated Protein Kinase in RAW264.7 Macrophages. *Food Chem.* **2012**, *135*, 967–975. [CrossRef] [PubMed]

76. Oliveira, T.; Figueiredo, C.A.; Brito, C.; Stavroullakis, A.; Prakki, A.; Da Silva Velozo, E.; Nogueira-Filho, G. Effect of *Allium cepa* L. on Lipopolysaccharide-Stimulated Osteoclast Precursor Cell Viability, Count, and Morphology Using 4′,6-Diamidino-2-Phenylindole-Staining. *Int. J. Cell Biol.* **2014**, *2014*, 535789. [CrossRef] [PubMed]

77. Main, K.A.; Mikelis, C.M.; Doçi, C.L. In Vitro Wound Healing Assays to Investigate Epidermal Migration. In *Methods in Molecular Biology*; Springer: New York, NY, USA, 2019; Volume 2109, pp. 147–154.

78. Martinotti, S.; Ranzato, E. Scratch Wound Healing Assay. In *Methods in Molecular Biology*; Springer: Berlin/Heidelberg, Germany, 2019; Volume 2109, pp. 225–229.

79. Jonkman, J.E.N.; Cathcart, J.A.; Xu, F.; Bartolini, M.E.; Amon, J.E.; Stevens, K.M.; Colarusso, P. An Introduction to the Wound Healing Assay Using Live-Cell Microscopy. *Cell Adhes. Migr.* **2014**, *8*, 440–451. [CrossRef]

80. Saitoh, M.; Kunitomo, J.; Kimura, E.; Hayase, Y.; Kobayashi, H.; Uchiyama, N.; Kawamoto, T.; Tanaka, T.; Mol, C.D.; Dougan, D.R.; et al. Design, Synthesis and Structure-Activity Relationships of 1,3,4-Oxadiazole Derivatives as Novel Inhibitors of Glycogen Synthase Kinase-3β. *Bioorg. Med. Chem.* **2009**, *17*, 2017–2029. [CrossRef]

81. Tauro, M.; Laghezza, A.; Loiodice, F.; Piemontese, L.; Caradonna, A.; Capelli, D.; Montanari, R.; Pochetti, G.; Di Pizio, A.; Agamennone, M.; et al. Catechol-Based Matrix Metalloproteinase Inhibitors with Additional Antioxidative Activity. *J. Enzym. Inhib. Med. Chem.* **2016**, *31*, 25–37. [CrossRef]

82. Xue, F.; Huang, J.; Ji, H.; Fang, J.; Li, H.; Martásek, P.; Roman, L.J.; Poulos, T.L.; Silverman, R.B. Structure-Based Design, Synthesis, and Biological Evaluation of Lipophilic-Tailed Monocationic Inhibitors of Neuronal Nitric Oxide Synthase. *Bioorg. Med. Chem.* **2010**, *18*, 6526–6537. [CrossRef]

83. Vilar, S.; Cozza, G.; Moro, S. Medicinal Chemistry and the Molecular Operating Environment (MOE): Application of QSAR and Molecular Docking to Drug Discovery. *Curr. Top. Med. Chem.* **2008**, *8*, 1555–1572. [CrossRef]